University of Reading

Numerical Schemes Applied to the Burgers and Buckley-Leverett Equations

by

Rakib Ahmed

September 2004

Department of Mathematics

Submitted to the Department of Mathematics, University of Reading, in partial fulfilment of the requirements for the Degree of Master of Science.

Acknowledgements

I would like to thank my supervisor Professor Mike Baines for his support and patience throughout the duration of this dissertation. I would also like to thank Dr Peter Sweby, Mark Wakefield, Paul Jelfs, Sue Davis and the postgraduate students in the department, for their assistance and encouragement.

Many thanks also go to the EPSRC for the scholorship which enabled the financial support throughtout this course.

Finally I would like to thank my family and friends for their love and support.

Declaration

I confirm that this is my own work and the use of all materials from other sources has been properly and fully acknowledged.

Signed

Abstract

In this dissertation we look at various classical numerical schemes which enable us to solve non-linear hyperbolic equations numerically. The first order upwind, Lax-Friedrichs, Lax-Wendroff and Warming-Beam schemes are used to solve the Burgers and the Buckley-Leverett equations to improve our understanding of the numerical diffusion and oscillations that can be present when using such schemes. For these equations we shall use characteristics to evaluate the exact solutions. By using different initial conditions we will look at situations where pure shocks are present, and also the case where both shocks and expansion fans are present, for both of the equations mentioned. The Buckley-Leverett case is slightly more complex and interesting because it has a non-convex flux function. We also briefly look at the Runge-Kutta Discontinuous Galerkin method, to consider a second order non-classical method, which does not produce oscillations.

Contents

Chapter 1

Introduction

Consider the hyperbolic conservation law

$$u_t + f(u)_x = 0 \tag{1.1}$$

where u is the conserved quantity and $f(u)$ is the flux. Applications of such equation can appear in the study of oil recovery, flow of gas, water, traffic flow, etc. We consider Burgers equation, where flux function $f(u) = \frac{1}{2}u^2$ and the Buckley-Leverett equation where $f(u) = \left(\frac{u^2}{u^2+\frac{1}{4}(1-u)^2}\right)$. Burgers equation in conservative form can be written as

$$u_t + \left(\frac{1}{2}u^2\right)_x = 0 \tag{1.2}$$

(ignoring any physical diffusion) and the Buckley-Leverett equation can be written as

$$u_t + \left(\frac{u^2}{u^2 + \frac{1}{4}(1-u)^2}\right)_x = 0 \tag{1.3}$$

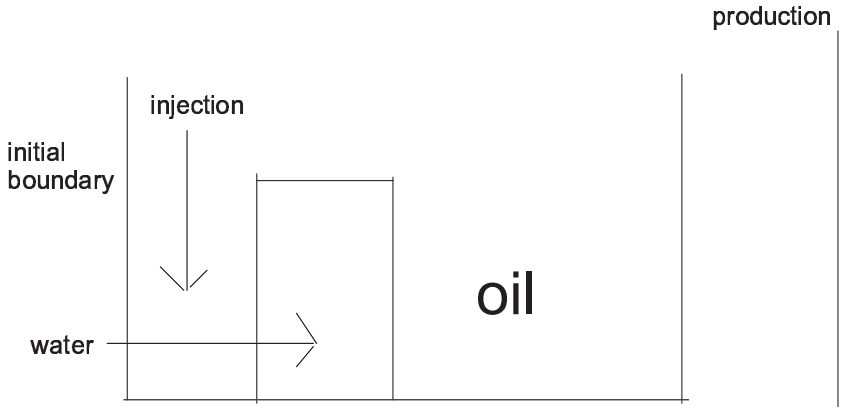

Figure 1.1: Sketch to show the basic technique

The Buckley-Leverett equation is used for oil recovery in industry. The discovery and recovery of oil is highly complex process, in which mathematical modelling and numerical simulation play a crucial role. Usually when an oil well is produced, the pressure at early stage is naturally high, and is such that there will be minimum difficulty in recovering the oil. The rate at which oil flows out of the well will naturally diminish with time; common ways of keeping up the oil flowing is to inject water to drive the oil towards the producing well.

Generally an oil reservoir consists of layers of porous rock, which are sandwiched between layers of impervious rock. These layers are often bent up in a cup shape which is known as an anticline. The oil reservoir is formed when oil is produced over geological time scales at great depths, migrating into a reservoir which is filled with water. This movement causes displacement to the water; gas may also be present depending on the pressure conditions. If gas is present then this forms a gas cap on top of the oil in the recovery of the solution. The proportion of oil, gas and

water which are present are known as saturations. In equation (1.3) there are two saturations present, water and oil: one of these saturations is u.

Using conservation laws we should note that convergence properties of numerical schemes can be severely damaged if discontinuties are present, which will affect the solution. Also numerical schemes can generate oscillations, whilst the analytic solutions do not have any. Classical numerical schemes such as first order upwind, Lax Friedrichs, Lax Wendroff and Warming-Beam are known as Finite Difference Methods, because the derivatives are approximated by differences of discrete values. It is a well known fact that the Lax Wendroff and Warming-Beam schemes cause oscillations at shocks, where steep gradients are present, whilst the other two schemes suffer from numerical diffusion. Here we confirm what they do at shocks, and also investigate what they do for a shock and fan combination, for the Buckley - Leverett equation.

Chapter 2 contains analytic solutions to the two equations obtained by using characteristics. We apply different initial/boundary conditions to the Burgers and Buckley-Leverett equations, to obtain shocks and rarefractions. In chapter 3 we introduce the classical numerical schemes that are used to solve the two equations numerically. We also look at the CFL condition which is necessary for such schemes to be stable and the role of the Modified Equation. In chapter 4 we briefly look at the Runge-Kutta Discontinuous Galerkin method applied to the Buckley-Leverett equation, demonstrating the basic derivation. Chapter 5 visualizes the results that are obtained by applying the numerical schemes. Finally chapter 6 will outline the conclusions which are drawn from the results of these numerical schemes.

Chapter 2

Exact Solution by Characteristics

Consider the hyperbolic conservation law

$$u_t + f(u)_x = 0 \tag{2.1}$$

where $f(u)$ is the flux function. This can also be written as

$$u_t + a(u)u_x = 0$$

where

$$a(u) = f'(u).$$

A basic solution procedure for hyperbolic equations is the method of characteristics, which will allow us to investigate the features of the solution of this equation. The characteristics are given by

$$\frac{dx}{dt} = a(u), \;\; on \;\; which \;\; \frac{du}{dt} = 0 \tag{2.2}$$

We can see that on the characteristics u is a constant, $u = u_0$ say. To obtain an equation for the characteristics we evaluate x as a function of t from

$$\frac{dx}{dt} = a(u_0) \tag{2.3}$$

giving

$$x = a(u_0)(t - t_0) + x_0 \tag{2.4}$$

The characteristics are given by equation 2.4.

2.1 Burgers' Equation

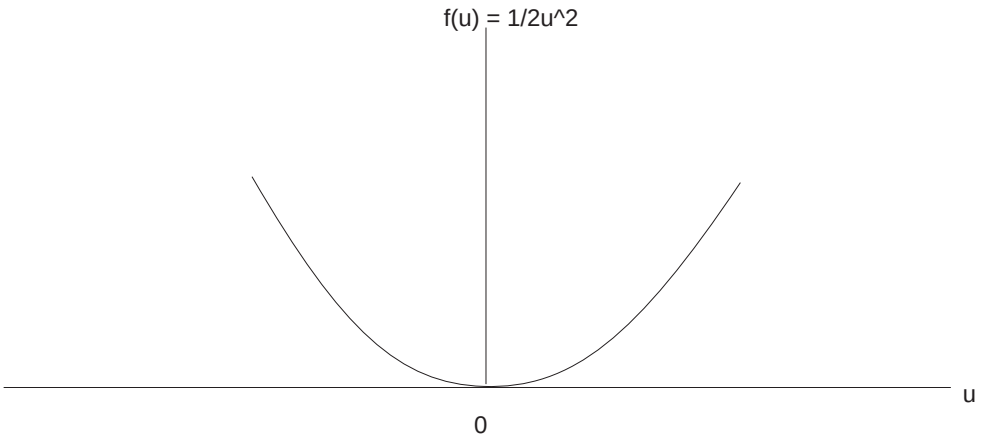

Figure 2.1: To show the shape of Burgers' equation

Introducing the flux of the Burgers equation [1] into equation 2.1 given above, we obtain

$$u_t + \left(\frac{1}{2}u^2\right)_x = 0 \tag{2.5}$$

Here

$$f(u) = \frac{1}{2}u^2 \qquad and \qquad a(u) = u$$

where $f(u)$ has a convex shape (see Fig. 2.2). Then

$$\frac{du}{dt} = 0 \qquad and \qquad \frac{dx}{dt} = u \Rightarrow \begin{cases} u = u_0 \\ x = u_0(t - t_0) + x_0 \end{cases} \tag{2.6}$$

2.1.1 Entropy Condition

A simple form of the entropy condition [13] states that for the condition to be valid, the characteristics can only enter the shock, whilst the characteristics cannot emerge away from the shock. This condition can be expressed algebraically, the entropy condition being written as

$$a(u_L) = f\prime(u_L) \geq \frac{f(u_R) - f(u_L)}{(u_R) - (u_L)} \geq f\prime(u_R) = a(u_R) \tag{2.65}$$

Note that the middle term in equation (2.65) is the slope of the chord joining u_L to u_R. This slope has to be greater than slope at u_R and less than slope at u_L.

2.1.2 Initial Data 1

We first use the initial data (in the right half of the plane)

$$u(x,0) = \begin{cases} \frac{1}{2} & x = 0 \\ 0 & x > 0 \qquad \forall t \end{cases}$$

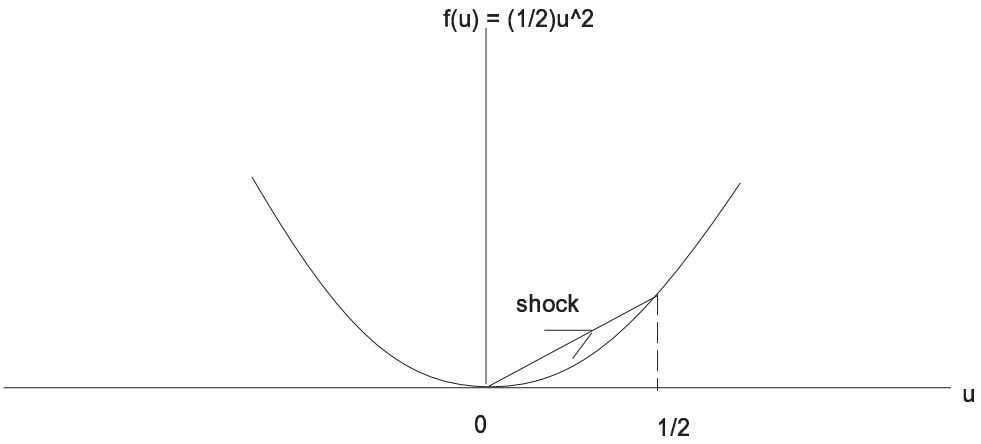

Figure 2.2: Shape of $f(u)$ for Burgers' equation with initial data 1 points

The characteristics are given by

$$\frac{du}{dt} = 0, \qquad \frac{dx}{dt} = u \Rightarrow \begin{cases} u = u_0 \\ x = u_0 t + x_0 \qquad (leaving\ the\ x-axis) \\ x = u_0(t - t_0) \qquad (leaving\ the\ t-axis) \end{cases} \tag{2.7}$$

Here

$$\frac{dx}{dt} = \begin{cases} \frac{1}{2} & \left(u = \frac{1}{2}\right) \quad for \quad t > 0 \quad x > 0 \\ 0 & \left(u = 0\right) \quad for \quad x > 0, \quad t > 0 \end{cases} \tag{2.8}$$

until they cross. Integrating equation (2.8), we obtain

$$x = \begin{cases} \frac{1}{2}\Big(t - t_0\Big) & when \quad t > 0, \quad x > 0 \\ x_0 & when \quad x > 0, \quad t > 0 \end{cases} \tag{2.9}$$

which agrees with equation (2.4). We can clearly see that the characteristics initially cross at $x = 0$ when $t = 0$. Therefore at the time $t = 0$ a discontinuity forms. To calculate the shock speed we use the Rankine-Hugoniot jump condition, obtaining

$$S = \frac{[f]}{[u]} = \frac{\frac{1}{2}\big(\frac{1}{2}\big)^2 - \frac{1}{2}\big(0\big)^2}{\frac{1}{2} - 0} = \frac{1}{4} \tag{2.10}$$

We therefore obtain the shock speed, which is $\frac{1}{4}$. Hence the solution is given by

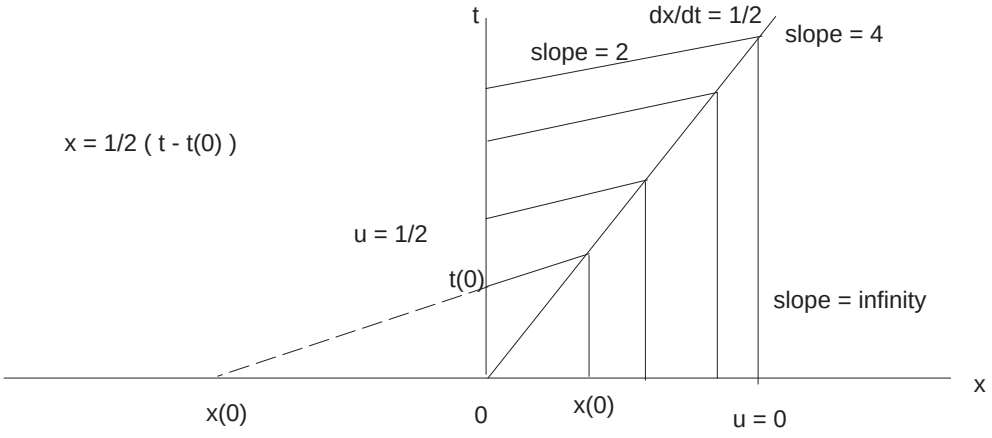

Figure 2.3: Characteristics for Burgers' equation with initial data 1

$$u = \begin{cases} \frac{1}{2} & in \quad t > 0, \quad x < \frac{1}{4}t \\ 0 & in \quad t > 0, \quad x > \frac{1}{4}t \end{cases} \tag{2.11}$$

(see Fig. 2.3).

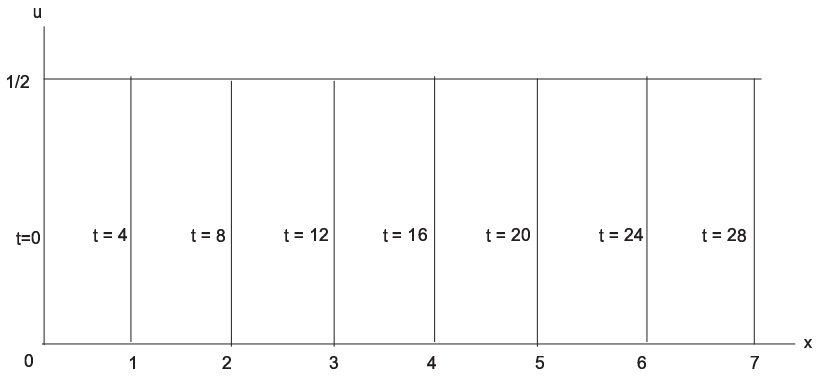

Figure 2.4: Graph to show solution at intervals of t =4, for example 1

2.1.3 Initial Data 2

Secondly we use the initial data (on the whole x-axis)

$$u(x,0) = \begin{cases} 0 & x < -1 \\ \frac{1}{2} & -1 < x < 0 \\ 0 & x > 0 \end{cases}$$

To evaluate the characteristics in the x,t plane for all $t > 0$, we proceed as follows. The characteristics are given by

$$\frac{du}{dt} = 0, \qquad \frac{dx}{dt} = u_0 = \begin{cases} 0 & x_0 < -1 \\ \frac{1}{2} & -1 < x_0 < 0 \\ 0 & x_0 > 0 \end{cases} \tag{2.12}$$

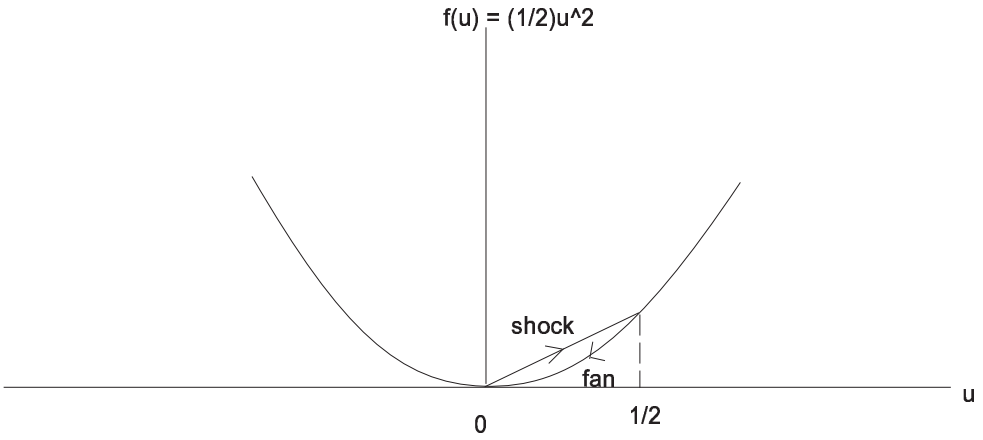

Figure 2.5: Flux function for Burgers' equation with initial data 2 points

i.e

$$\frac{dx}{dt} = \begin{cases} 0 & \big(u = 0\big) \quad for \quad x < -1, \quad t > 0. \\ \frac{1}{2} & \big(u = \frac{1}{2}\big) \quad for \quad t > 0 \quad -1 \leq x \leq 0 \\ 0 & \big(u = 0\big) \quad for \quad x > 0, \quad t > 0. \end{cases} \tag{2.13}$$

until they cross. Integrating equation (2.13), we obtain

$$x = \begin{cases} x_0 & when \quad x < -1, \quad t > 0 \\ \frac{1}{2}\Big(t - t_0\Big) & when \quad -1 \leq x \leq 0, \quad t > 0 \\ x_0 & when \quad x > 0, \quad t > 0 \end{cases} \tag{2.14}$$

The shock is initially at $x = 0$. We proceed as follows to calculate the shock speed. As before

$$S = \frac{[f]}{[u]} = \frac{f_R - f_L}{u_R - u_L} = \frac{\frac{1}{2}\big(0\big)\big)^2 - \frac{1}{2}\big(\frac{1}{2}\big)^2}{0 - \frac{1}{2}} = \frac{1}{4} \tag{2.15}$$

Connecting $(0, 0)$ to $(0, \frac{1}{2})$ is a straight line which represents the shock. By looking

at Figure (2.5) we can visualise that by connecting $\frac{1}{2}$ to 0 on the curve represents the fan. The initial shock for this problem is at $x = 0$ with a speed which is $\frac{1}{4}$. Using this we obtain the shock line $x_s(t)$ which is

$$x_s = 0 + \frac{1}{4}t = \frac{1}{4}t \tag{2.16}$$

To satisfy the entropy condition we now have to fill the 'void' with a characteristic fan, which is given by [13]

$$\frac{dx}{dt} = A = \frac{(x+1)}{t},$$

hence

$$x + 1 = At \qquad , \qquad 0 \leq A \leq \frac{1}{2}$$

The part of the expansion when $A = \frac{1}{2}$ reaches the shock when

$$-1 + \frac{1}{2}t = \frac{1}{4}t \tag{2.17}$$

The left hand side of the equation (2.17) was obtained from the fan, which is due to the top of expansion wave having $u = \frac{1}{2}$ at $x = -1$ prior to the shock meeting. The right hand side was obtained from the shock. Solving equation (2.17) gives rise to

$$t\Big(\frac{1}{4} - \frac{1}{2}\Big) = -1 \qquad \Rightarrow t = 4$$

Therefore when $t \leq 4$, we have $u = 0$ for both cases when $x < -1$ and for $x > 0$ to the right of the shock, $u = \frac{1}{2}$ to the left of the shock while in the region $-1 < x < t$ we have

$$u(x,t) = \frac{x+1}{t}$$

Hence for $t \leq 4$ we have

$$u(x,t) = \begin{cases} 0 & x < -1 \\ \frac{x+1}{t} & -1 < x < \frac{t}{2} - 1 \\ \frac{1}{2} & \frac{t}{2} - 1 < x < \frac{1}{4}t \\ 0 & \frac{1}{4}t < x \end{cases} \tag{2.18}$$

(see Figure 2.6). We now look at the form of the shock when the expansion meets

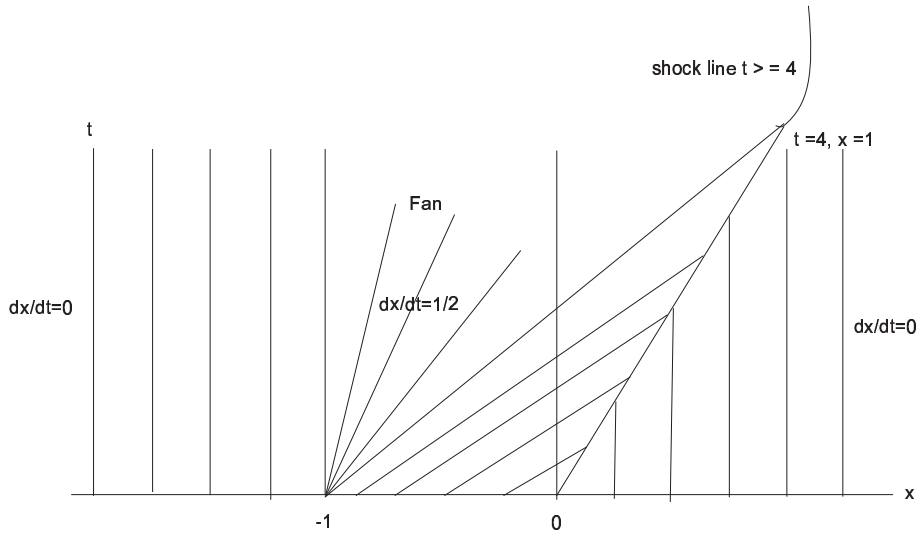

Figure 2.6: Burgers' equation for example 2

the shock $t \geq 4$. To do this we equate the shock speed to the average of the values to the left and to the right:

$$\frac{dx_s}{dt} = \frac{1}{2}\Big(u_R + u_L\Big) = \frac{1}{2}\left(\frac{(x_s+1)}{t} + 0\right)$$

i.e.

$$S = \frac{dx_s}{dt} = \frac{(x_s+1)}{2t} \tag{2.19}$$

From equation (2.16) we can see that the ODE is separable, giving rise to

$$\int \frac{dx_s}{x_s + 1} = \int \frac{dt}{2t}$$

$$ln\ (x_s + 1) = \frac{1}{2} ln\ t + log\ B$$

$$x_s + 1 = Bt^{\frac{1}{2}} \tag{2.20}$$

We know that the shock passes through the point $t = 4$ at $x = 1$. Using this information we find that $B = 1$. Therefore we have now evaluated the shock path for $t \geq 4$, which is

$$x_s = -1 + \sqrt{t} \tag{2.21}$$

2.2 Buckley-Leverett Equation

Now consider again the general form of the one-dimensional hyperbolic conservation law as given by equation (2.1), and implement the flux of the Buckley-Leverett equation [1]. We obtain

$$u_t + \left(\frac{u^2}{u^2 + \frac{1}{4}(1-u)^2} \right)_x = 0, \qquad \forall x \in \mathbf{R} \tag{2.22}$$

The flux function is now non-convex (the graph has an S shape) as sketched in figure 2.6. To evaluate $a(u)$, we use the quotient rule, giving

$$a(u) = f'(u) = \frac{\Big(5u^2 - 2u + 1\Big)8u - 4u^2\Big(10u - 2\Big)}{\Big(5u^2 - 2u + 1\Big)^2} = \frac{\Big(8u - 8u^2\Big)}{\Big(5u^2 - 2u + 1\Big)^2}$$

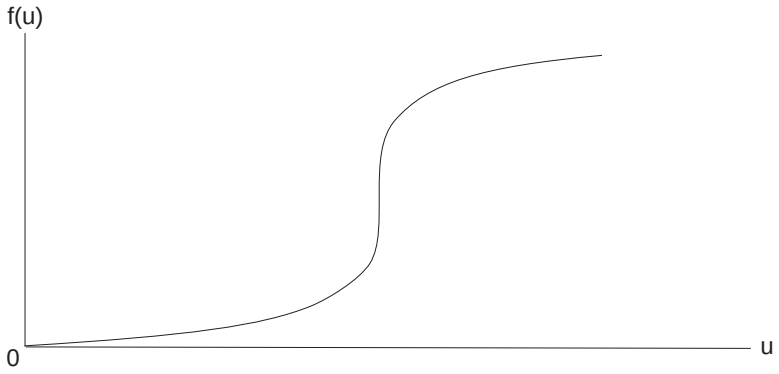

Figure 2.7: To show the shape of a non-convex function

2.2.1 Initial Data 1 for the B-L equation

In this problem we will again use the initial data

$$u(x,0) = \begin{cases} \frac{1}{2} & x = 0 \\ 0 & x > 0 \end{cases}$$

To evaluate the characteristics in the x,t plane for all $t > 0$, we proceed as follows. The characteristics are given by

$$\frac{dx}{dt} = a(u), \qquad \frac{du}{dt} = 0 \tag{2.23}$$

We can see that u is a constant which shall be denoted by u_0. From equation (2.23), $u = u_0$ and x is given by

$$x = a(u_0)t + x_0 \tag{2.24}$$

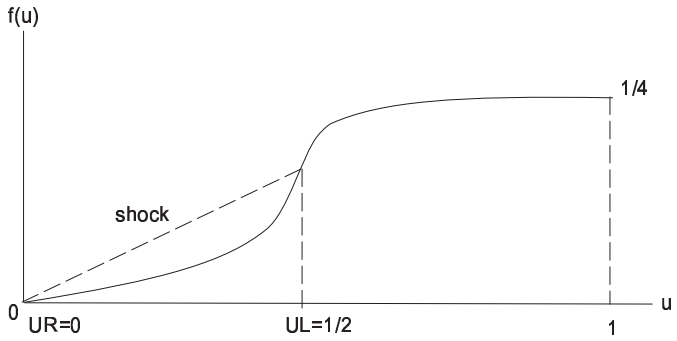

Figure 2.8: Graph of B-L flux and shock construction for first initial conditions

where

$$a(u_0) = \frac{\Big(5u_0^2 - 2u_0 + 1\Big)8u_0 - 4u_0^2\Big(10u_0 - 2\Big)}{\Big(5u_0^2 - 2u_0 + 1\Big)^2}$$

Hence

$$\frac{dx}{dt} = a(u_0) = \frac{\Big(8u_0 - 8u_0^2\Big)}{\Big(5u_0^2 - 2u_0 + 1\Big)^2}$$

The characteristics are now

$$x = \left(\frac{8u_0 - 8u_0^2}{\big(5u_0^2 - 2u_0 + 1\big)^2}\right)t + x_0 \tag{2.25}$$

We can substitute the initial conditions into equation (2.25), giving

$$x = \begin{cases} \frac{32}{25}t & x_0 = 0 \qquad (leaving\ the\ t-axis) \\ x_0 & x_0 > 0 \qquad (leaving\ the\ x-axis) \end{cases}$$

At $x = t = 0$ the characteristic cross, the partial differential equation breaks down

and we have the shock speed

$$\frac{dx_s}{dt} = \frac{f_R - f_L}{u_R - u_L} = \frac{0 - \left(\frac{\frac{1}{4}}{\frac{1}{4}+\frac{1}{4}\left(1-\frac{1}{2}\right)^2}\right)}{0 - \frac{1}{2}} = \frac{8}{5}$$

For this initial condition we always get a shock, see figure (2.8). By looking at this figure we can see that the line connecting the points is a straight line, which satisfies the entropy condition, see equation (2.65).

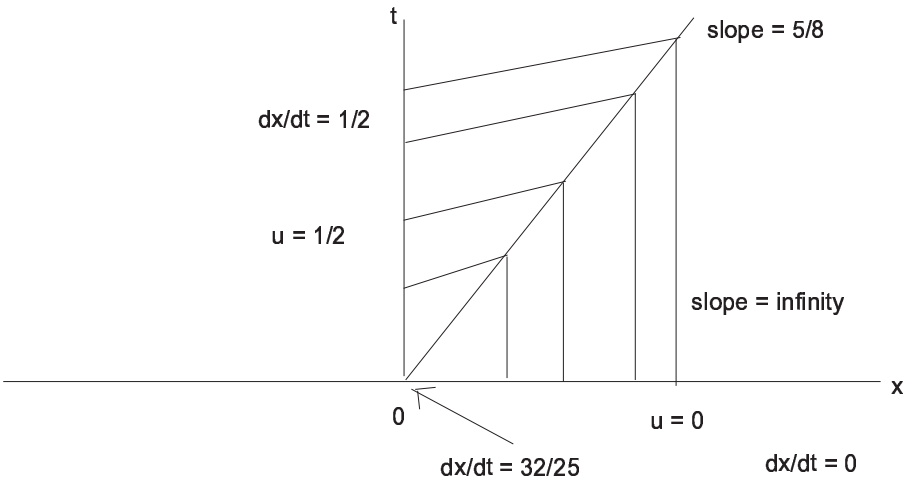

Figure 2.9: Characteristic diagram for the Buckley-Leverett equation for example 1

2.2.2 Initial Data 2 for the B-L equation

The second example has the initial conditions

$$u(x,0) = \begin{cases} \frac{3}{4} & x = 0 \\ 0 & x > 0 \end{cases}$$

Evaluating the characteristics in the x,t plane for all $t > 0$, we obtain (as before)

$$x = \left(\frac{8u_0 - 8u_0^2}{\left(5u_0^2 - 2u_0 + 1\right)^2} \right) t + x_0 \tag{2.26}$$

This time we get not only a shock but also a fan (see Figure 2.10) because we

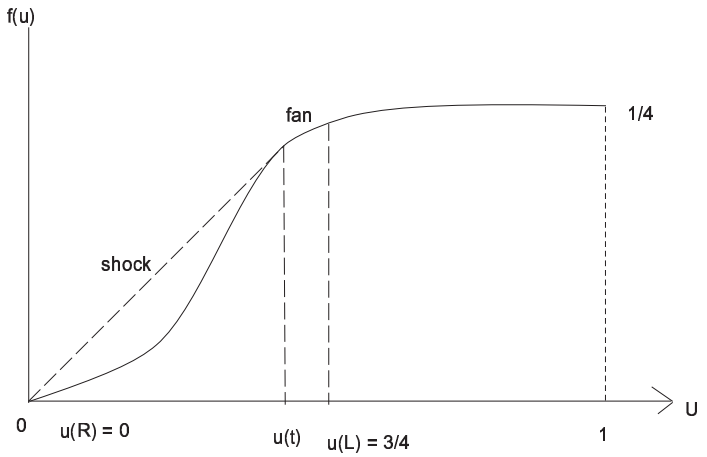

Figure 2.10: Buckley-Leverett equation for example 2

cannot connect the points $(0, 0)$ and $(\frac{3}{4}, f(\frac{3}{4}))$ by a straight line, and satisfy the entropy condition see equation (2.65). Instead let u_T the value of u corresponding to the tangent from $(0, 0)$ to the curve. To evaluate u_T, we proceed as follows:

The slope of curve at u_T must equal slope of tangent at u_T, therefore

$$f^{'}(u_T) = \frac{f(u_T) - 0}{u_T - 0} \tag{2.27}$$

which leads to

$$\frac{8u_T - 8u_T^2}{\left(5u_T^2 - 2u_T + 1\right)^2} = \frac{u_T^2 + \frac{1}{4}\left(1 - u_T\right)^2}{u_T} \tag{2.28}$$

Therefore u_T is given by equation (2.28). This is a non-linear equation for u_T. In order to use Newton's method to solve equation (2.28) we re-arrange it to obtain in the form $F(u_T) = 0$ to, where $F(u_T)$ is

$$F(u_t) = \frac{8u_T - 8u_T^2}{\left(5u_T^2 - 2u_T + 1\right)^2} - \frac{u_T^2 + \frac{1}{4}\left(1 - u_T\right)^2}{u_T} \tag{2.29}$$

The method is described in terms of a sequence, using the Newton formula

$$x_{n+1} = x_n - \frac{F(x_n)}{F'(x_n)} \tag{2.30}$$

By starting with an initial guess of $\frac{1}{2}$, we obtain the value of u_T after 5 iterations where $u_T = 0.617403$. The actual form of fan is beyond the scope of this work, so it is just sketched.

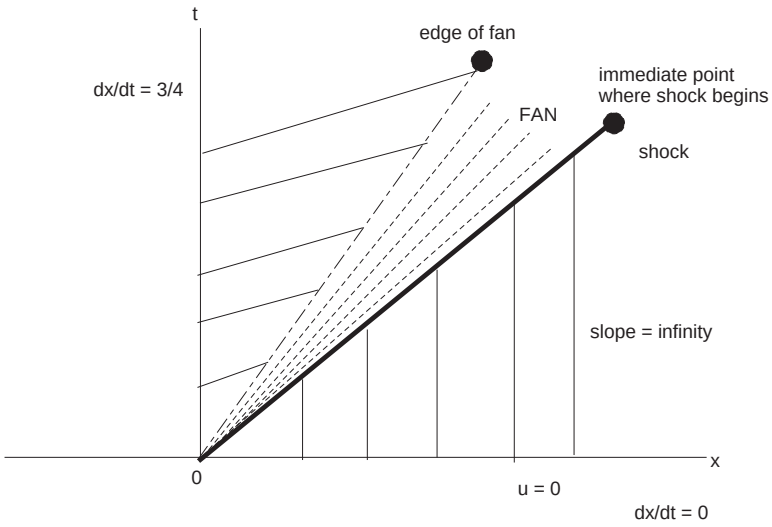

Figure 2.11: Sketch of characteristic diagram for the Buckley-Leverett equation

Chapter 3

Classical numerical schemes

Consider the general form of the hyperbolic conservation law given by equation (2.1). In our case the two non-linear equations used are the Burgers and the Buckley-Leverett equations. The flux of the equations are given by $f(u) = \frac{1}{2}u^2$, and $f(u) = \left(\frac{u^2}{u^2+\frac{1}{4}(1-u)^2}\right)$, respectively. We now turn our attention to the numerical approximation of the solutions of the equations mentioned above. We should note that there are a vast amount of numerical techniques which can be used to approximate conservation laws but we shall concentrate on the Finite Difference Methods. When using finite difference methods the derivatives are approximated by differences. The four numerical schemes we shall consider are the Lax-Friedrichs, first order upwind, Lax-Wendroff and Warming-Beam.

We can write conservative finite difference schemes for solving the conservation law in the explicit form

$$u_j^{n+1} = u_j^n - \frac{\Delta t}{\Delta x}\left(h_{j+\frac{1}{2}}^n - h_{j-\frac{1}{2}}^n\right) \tag{3.1}$$

where

$$h^n_{j+\frac{1}{2}} = h\Big(u^n_{j-1}, ..., u^n_{j+r}\Big) \tag{3.2}$$

Here h is a consistent numerical flux function and $u^n_j = u\big(j\Delta x, n\Delta t\big)$. We should note that many different numerical schemes have been developed to overcome some of the difficulties that are faced when dealing with the numerical simulation of conservation laws.

3.1 The CFL condition

In order to have stability when using explicit numerical schemes, we are required to apply the necessary condition known as the Courant-Friedrichs-Lewy condition. It is often referred to as the CFL or Courant condition, [9] and [12], and is

$$\mu = \left| a\frac{\Delta t}{\Delta x} \right| \leq 1 \tag{3.3}$$

where $a = a(u) = \frac{\partial f}{\partial u}$, which represents a wave speed. Here Δt and Δx are the time and space steps, respectively. If a small space step is used then a small time step is needed to keep the numerical simulation stable. This condition is not sufficient for stability, as it is only a necessary condition for a scheme to be stable. Once the scheme has satisfied the CFL condition, it can then be considered in more depth by using a stability test which is sufficient.

3.2 Lax-Friedrichs

The Lax Friedrichs scheme is first order accurate in both space and time, and the stability region is defined by $\left|a\frac{\Delta t}{\Delta x}\right| \leq 1$. The picture on the right of figure (3.1)

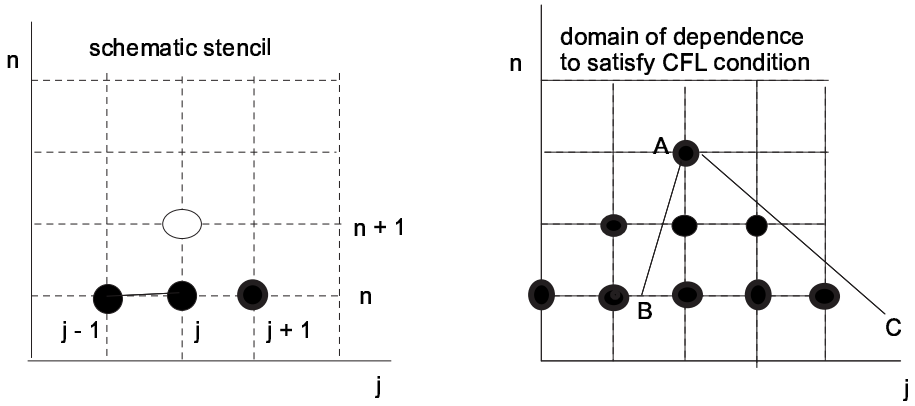

Figure 3.1: Stencils for the lax friedrichs scheme

shows the domain of dependence. If $a\frac{\Delta t}{\Delta x}$ is slope of AB then the CFL condition is satisfied because AB lies in the stencil of the scheme, whilst the line AC is a violation of the CFL condition, lying outside the domain of dependence. The numerical flux function is given by

$$h^n_{j+\frac{1}{2}} = \frac{1}{2}\Big(f_j + f_{j+1}\Big) - \frac{\Delta x}{2\Delta t}\Big(u^n_{j+1} - u^n_j\Big), \tag{3.4}$$

where f is the the flux of the equation we are going to use. If we substitute the flux of Burgers' equation into equation (3.4), we obtain.

$$h^n_{j+\frac{1}{2}} = \frac{1}{2}\left(\frac{1}{2}u^2_j + \frac{1}{2}u^2_{j+1}\right) - \frac{\Delta x}{2\Delta t}\Big(u^n_{j+1} - u^n_j\Big) \tag{3.5}$$

and

$$h^n_{j-\frac{1}{2}} = \frac{1}{2}\left(\frac{1}{2}u^2_{j-1} + \frac{1}{2}u^2_j\right) - \frac{\Delta x}{2\Delta t}\left(u^n_j - u^n_{j-1}\right) \tag{3.6}$$

We can now write down the Lax-Friedrichs conservative finite difference scheme for solving the conservation law for the Burgers equation in its conservative form by substituting equation (3.5) and (3.6) into equation (3.1). Doing this we obtain.

$$u^{n+1}_j = u^n_j - \frac{\Delta t}{\Delta x}\left(\left(\frac{1}{2}\left(\frac{1}{2}u^2_j + \frac{1}{2}u^2_{j+1}\right) - \frac{\Delta x}{2\Delta t}\left(u^n_{j+1} - u^n_j\right)\right)\right.$$

$$\left. -\left(\frac{1}{2}\left(\frac{1}{2}u^2_{j-1} + \frac{1}{2}u^2_j\right) - \frac{\Delta x}{2\Delta t}\left(u^n_j - u^n_{j-1}\right)\right)\right) \tag{3.7}$$

and simplifying equation (3.7) gives

$$u^{n+1}_j = u^n_j - \frac{\Delta t}{4\Delta x}\left(u^2_{j+1} + u^2_{j-1}\right) + \frac{1}{2}\left(u^n_{j+1} + u^n_{j-1}\right) \tag{3.8}$$

By substituting the flux of the Buckley-Leverett equation into equation (3.4), we get

$$h^n_{j+\frac{1}{2}} = \frac{1}{2}\left(\frac{u^2_j}{u^2_j + \frac{1}{4}\left(1-u_j\right)^2} + \frac{u^2_{j+1}}{u^2_{j+1} + \frac{1}{4}\left(1-u_{j+1}\right)^2}\right) - \frac{\Delta x}{2\Delta t}\left(u^n_{j+1} - u^n_j\right) \tag{3.9}$$

and

$$h^n_{j-\frac{1}{2}} = \frac{1}{2}\left(\frac{u^2_{j-1}}{u^2_{j-1} + \frac{1}{4}\left(1-u_{j-1}\right)^2} + \frac{u^2_j}{u^2_j + \frac{1}{4}\left(1-u_j\right)^2}\right) - \frac{\Delta x}{2\Delta t}\left(u^n_j - u^n_{j-1}\right) \tag{3.10}$$

We can now write down the Lax-Friedrichs conservative finite difference scheme for solving the conservation law for the Buckley-Leverett equation in its conservative

form by substituting equation (3.9) and (3.10) into equation (3.1), leads to

$$u_j^{n+1} = u_j^n - \frac{\Delta t}{\Delta x}\left(\left(\frac{1}{2}\left(\frac{u_j^2}{u_j^2 + \frac{1}{4}\left(1-u_j\right)^2} + \frac{u_{j+1}^2}{u_{j+1}^2 + \frac{1}{4}\left(1-u_{j+1}\right)^2}\right) - \frac{\Delta x}{2\Delta t}\left(u_{j+1}^n - u_j^n\right)\right)\right.$$

$$\left. - \left(\frac{1}{2}\left(\frac{u_{j-1}^2}{u_{j-1}^2 + \frac{1}{4}\left(1-u_{j-1}\right)^2} + \frac{u_j^2}{u_j^2 + \frac{1}{4}\left(1-u_j\right)^2}\right) - \frac{\Delta x}{2\Delta t}\left(u_j^n - u_{j-1}^n\right)\right)\right) \quad (3.11)$$

and simplifying equation (3.11) gives

$$u_j^{n+1} = u_j^n - \frac{\Delta t}{2\Delta x}\left(\frac{u_{j+1}^2}{u_{j+1}^2 + \frac{1}{4}\left(1-u_{j+1}\right)^2} - \frac{u_{j-1}^2}{u_{j-1}^2 + \frac{1}{4}\left(1-u_{j-1}\right)^2}\right)$$

$$+\frac{1}{2}\left(u_{j+1}^n + u_{j-1}^n\right) \quad (3.12)$$

The Lax-Friedrichs scheme has now been written in its conservative form for the Burgers and the Buckley-Leverett equations.

3.3 First order upwind

The first order upwind scheme is also first order accurate in both space and time, but the scheme is only stable for the interval $0 \leq a\frac{\Delta t}{\Delta x} \leq 1$ for $(a > 0)$, or $-1 \leq a\frac{\Delta t}{\Delta x} \leq 0$ for $(a < 0)$.

The picture on the right of figure (3.2) also shows the domain of dependence. If $a\frac{\Delta t}{\Delta x}$ is slope of AB then the CFL condition is satisfied because AB lies in the stencil of the scheme, whilst the line AC is a violation of the CFL condition, lying outside the domain of dependence. The numerical flux function is

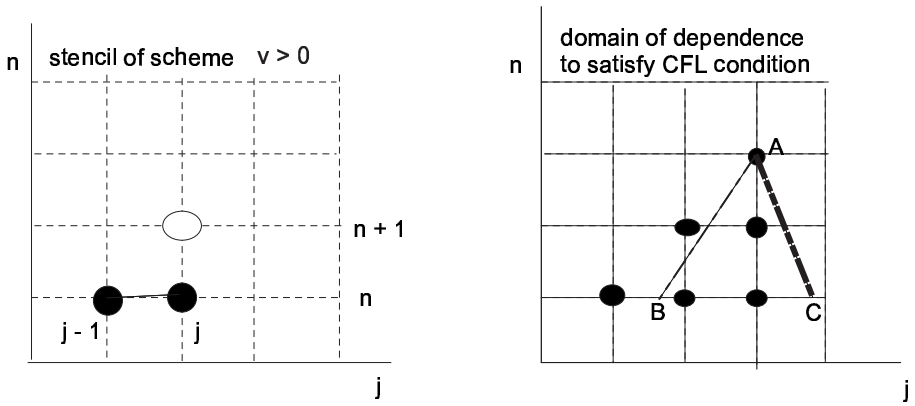

Figure 3.2: Stencils for the first order Upwind scheme

$$h_{j+\frac{1}{2}} = \begin{cases} f_j & v_{j+\frac{1}{2}} > 0 \\ f_{j+1} & v_{j+\frac{1}{2}} < 0 \end{cases} \tag{3.13}$$

where

$$v_{j+\frac{1}{2}} = \begin{cases} \frac{\Delta t}{\Delta x}\frac{f_{j+1}-f_j}{u_{j+1}-u_j} & u_j \neq u_{j+1} \\ \frac{\Delta t}{\Delta x} f\prime(u_j) & u_j = u_{j+1} \end{cases} \tag{3.14}$$

Applying the Burgers flux to the first order Upwind scheme, $h_{j+\frac{1}{2}}$ gives rise to

$$h_{j+\frac{1}{2}} = \begin{cases} \frac{1}{2}u_j^2 & v_{j+\frac{1}{2}} > 0 \\ \frac{1}{2}u_{j+1}^2 & v_{j+\frac{1}{2}} < 0 \end{cases} \tag{3.15}$$

where

$$v_{j+\frac{1}{2}} = \begin{cases} \frac{\Delta t}{\Delta x}\frac{1}{2}(u_{j+1}+u_j) & u_j \neq u_{j+1} \\ \frac{\Delta t}{\Delta x}u_j & u_j = u_{j+1} \end{cases}$$

For $h_{j-\frac{1}{2}}$, we obtain

$$h_{j-\frac{1}{2}} = \begin{cases} \frac{1}{2}u_{j-1}^2 & v_{j-\frac{1}{2}} > 0 \\ \frac{1}{2}u_j^2 & v_{j-\frac{1}{2}} < 0 \end{cases} \tag{3.16}$$

where

$$v_{j-\frac{1}{2}} = \begin{cases} \frac{\Delta t}{\Delta x}\frac{1}{2}(u_j + u_{j-1}) & u_{j-1} \neq u_j \\ \frac{\Delta t}{\Delta x}u_{j-1} & u_{j-1} = u_j \end{cases}$$

We can now write the first order upwind scheme for solving the conservation law, for the Burgers equation in its conservative form by substituting equation (3.15) and (3.16) into equation (3.1), which gives rise to

$$u_j^{n+1} = u_j^n - \frac{\Delta t}{\Delta x}\big(equation(3.15) - equation(3.16)\big) \tag{3.17}$$

Introducing the Buckley-Leverett flux into the first order upwind scheme, for $h_{j+\frac{1}{2}}$ we have

$$h_{j+\frac{1}{2}} = \begin{cases} \frac{u_j^2}{u_j^2+\frac{1}{4}(1-u_j)^2} & v_{j+\frac{1}{2}} > 0 \\ \frac{u_{j+1}^2}{u_{j+1}^2+\frac{1}{4}(1-u_{j+1})^2} & v_{j+\frac{1}{2}} < 0 \end{cases} \tag{3.18}$$

where

$$v_{j+\frac{1}{2}} = \begin{cases} \frac{\Delta t}{\Delta x}\frac{\frac{u_{j+1}^2}{u_{j+1}^2+\frac{1}{4}(1-u_{j+1})^2} - \frac{u_j^2}{u_j^2+\frac{1}{4}(1-u_j)^2}}{u_{j+1}-u_j} & u_j \neq u_{j+1} \\ \frac{\Delta t}{\Delta x}\frac{8u_j - 8u_j^2}{(5u_j^2-2u_j+1)^2} & u_j = u_{j+1} \end{cases}$$

For $h_{j-\frac{1}{2}}$ we obtain

$$h_{j-\frac{1}{2}} = \begin{cases} \frac{u_{j-1}^2}{u_{j-1}^2+\frac{1}{4}(1-u_{j-1})^2} & v_{j-\frac{1}{2}} > 0 \\ \frac{u_j^2}{u_j^2+\frac{1}{4}(1-u_j)^2} & v_{j-\frac{1}{2}} < 0 \end{cases} \tag{3.19}$$

where

$$v_{j-\frac{1}{2}} = \begin{cases} \frac{\Delta t}{\Delta x} \frac{\frac{u_j^2}{u_j^2+\frac{1}{4}(1-u_j)^2} - \frac{u_{j-1}^2}{u_{j-1}^2+\frac{1}{4}(1-u_{j-1})^2}}{u_j - u_{j-1}} & u_{j-1} \neq u_j \\ \frac{\Delta t}{\Delta x} \frac{8u_{j-1} - 8u_{j-1}^2}{(5u_{j-1}^2 - 2u_{j-1}+1)^2} & u_{j-1} = u_j \end{cases}$$

The scheme can now be written in conservarive form by substituting equation (3.18) and (3.19) into equation (3.1), giving rise to

$$u_j^{n+1} = u_j^n - \frac{\Delta t}{\Delta x}\big(equation(3.18) - equation(3.19)\big) \tag{3.20}$$

3.4 Lax-Wendroff

The Lax-Wendroff is a second order accurate scheme. This scheme is known to be stable for the region $\left|a\frac{\Delta t}{\Delta x}\right| \leq 1$. The picture on the right of figure (3.3) shows the

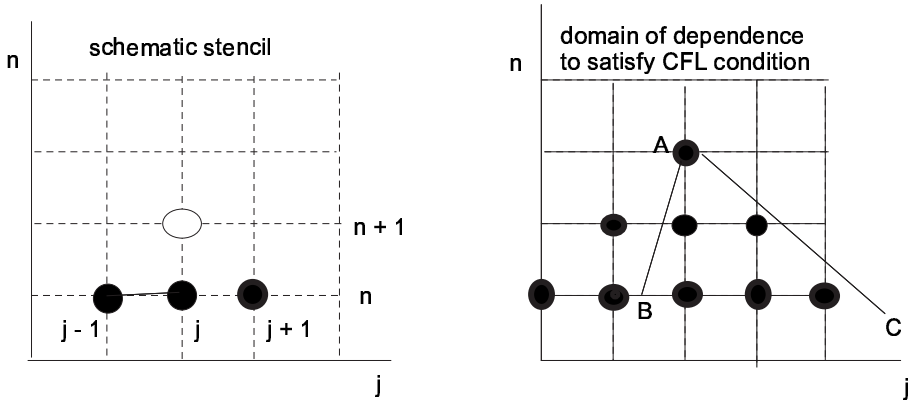

Figure 3.3: Stencils for the Lax-Wendroff scheme

domain of dependence for this numerical scheme. If $a\frac{\Delta t}{\Delta x}$ is the slope of AB then the CFL condition is satisfied because AB lies in the stencil of the scheme, whilst the

line AC violates the CFL condition, by lying outside the domain of dependence.

The numerical flux function can be written as

$$h_{j+\frac{1}{2}} = \frac{1}{2}\bigg((f_{j+1} + f_j) - v_{j+\frac{1}{2}}(f_{j+1} - f_j)\bigg) \tag{3.21}$$

Substituting the Burgers flux gives rise to

$$h_{j+\frac{1}{2}} = \frac{1}{2}\bigg((\frac{1}{2}u_{j+1}^2 + \frac{1}{2}u_j^2) - v_{j+\frac{1}{2}}(\frac{1}{2}u_{j+1}^2 - \frac{1}{2}u_j^2)\bigg) \tag{3.22}$$

$h_{j-\frac{1}{2}}$ leads to

$$h_{j-\frac{1}{2}} = \frac{1}{2}\bigg((\frac{1}{2}u_j^2 + \frac{1}{2}u_{j-1}^2) - v_{j-\frac{1}{2}}(\frac{1}{2}u_j^2 - \frac{1}{2}u_{j-1}^2)\bigg) \tag{3.23}$$

Introducing the Buckley-Leverett equation into the Lax-Wendroff scheme gives

$$\begin{aligned} h_{j+\frac{1}{2}} = \frac{1}{2}\bigg(&((\frac{u_{j+1}^2}{u_{j+1}^2 + \frac{1}{4}(1-u_{j+1})^2}) + (\frac{u_j^2}{u_j^2 + \frac{1}{4}(1-u_j)^2}))- \\ &v_{j+\frac{1}{2}}((\frac{u_{j+1}^2}{u_{j+1}^2 + \frac{1}{4}(1-u_{j+1})^2}) - (\frac{u_j^2}{u_j^2 + \frac{1}{4}(1-u_j)^2}))\bigg) \end{aligned} \tag{3.24}$$

and

$$\begin{aligned} h_{j-\frac{1}{2}} = \frac{1}{2}\bigg(&((\frac{u_j^2}{u_j^2 + \frac{1}{4}(1-u_j)^2}) + (\frac{u_{j-1}^2}{u_{j-1}^2 + \frac{1}{4}(1-u_{j-1})^2}))- \\ &v_{j-\frac{1}{2}}((\frac{u_j^2}{u_j^2 + \frac{1}{4}(1-u_j)^2}) - (\frac{u_{j-1}^2}{u_{j-1}^2 + \frac{1}{4}(1-u_{j-1})^2}))\bigg) \end{aligned} \tag{3.25}$$

where $v_{j-\frac{1}{2}}$ and $v_{j+\frac{1}{2}}$ for this scheme are as in the first order upwind scheme. We can now write the Lax-Wendroff scheme for solving the conservation law, for the Burgers and the Buckley-Leverett equations may be written as

$$u_j^{n+1} = u_j^n - \frac{\Delta t}{\Delta x}\big(equation(3.22) - equation(3.23)\big) \tag{3.26}$$

and

$$u_j^{n+1} = u_j^n - \frac{\Delta t}{\Delta x}\big(equation(3.24) - equation(3.25)\big) \tag{3.27}$$

3.5 Warming-Beam

The Warming-Beam is also a second order accurate numerical scheme, but the scheme is only stable for the interval $0 \leq a\frac{\Delta t}{\Delta x} \leq 2$.

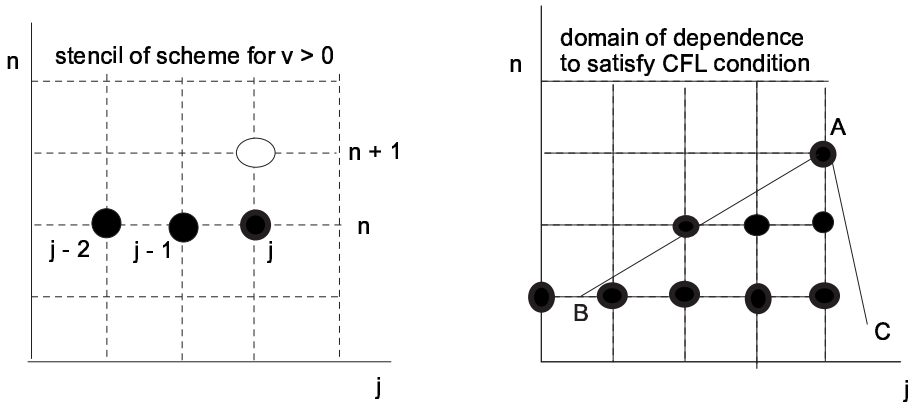

Figure 3.4: Stencils for the Warming-Beam scheme

The picture on the right of figure (3.4) shows the domain of dependence for this numerical scheme. If $a\frac{\Delta t}{\Delta x}$ is the slope of AB then the CFL condition is satisfied

because AB lies in the stencil of the scheme, whilst the line AC violates the CFL condition, by lying outside the domain of dependence. The numerical flux function can be written as

$$h_{j+\frac{1}{2}} = \begin{cases} \frac{1}{2}\big(3f_j - f_{j-1}\big) - \frac{1}{2}v_{j-\frac{1}{2}}\big(f_j - f_{j-1}\big) & v_{j+\frac{1}{2}} > 0 \\ \frac{1}{2}\big(3f_{j+1} - f_{j+2}\big) - \frac{1}{2}v_{j+\frac{3}{2}}\big(f_{j+2} - f_{j+1}\big) & v_{j+\frac{1}{2}} < 0 \end{cases} \tag{3.28}$$

and

$$h_{j-\frac{1}{2}} = \begin{cases} \frac{1}{2}\big(3f_{j-1} - f_{j-2}\big) - \frac{1}{2}v_{j-\frac{3}{2}}\big(f_{j-1} - f_{j-2}\big) & v_{j-\frac{1}{2}} > 0 \\ \frac{1}{2}\big(3f_j - f_{j+1}\big) - \frac{1}{2}v_{j+\frac{1}{2}}\big(f_{j+1} - f_j\big) & v_{j-\frac{1}{2}} < 0 \end{cases} \tag{3.29}$$

where $v_{j-\frac{1}{2}}$ and $v_{j+\frac{1}{2}}$ are as given in the first order upwind scheme. To write the Warming-Beam scheme in order to solve the conservation law for Burgers and Buckley-Leverett equations, we follow a procedure similar to the first order upwind scheme, which is described in section 3.3.

3.6 TVD and Limiters

Consider the Lax-Wendroff and Warming-Beam schemes, where oscillations are present to the left and right of the discontinuity, respectively. One reason for oscillations occurring is due to the numerical schemes not satisfying the maximum principle, see [1] and [12]. The local maximum principle (3 point Lax-Wendroff scheme) is given by

$$min\big(u_{j-1}^n, u_j^n, u_{j+1}^n\big) \leq u_j^{n+1} \leq max\big(u_{j-1}^n, u_j^n, u_{j+1}^n\big)$$

In the Lax-Wendroff and Warming-Beam schemes there are no implementation of

the TVD (total variation diminishing) property, which the original problem satisfies. The total variation $TV = \sum |u_{j+1}^n - u_j^n|$ and the D means it is decreasing in time (within). The introduction of flux limiters can be added to the Lax Wendroff and Warming-Beam schemes in order to make it TVD and therefore non-oscillatory. I have not pursued limiters for the finite difference methods here for the lack of time span, but I have included (in the next chapter) a description of the RKDG method which I studied last year and does have a TVD property built in.

3.7 Modified Equation

In order to analyse finite difference methods, we note that to every finite difference approximation is of order $\bigcirc(\Delta t^R, \Delta x^S)$ for a given differential equation. There is another differential equation which is known as the Modified Equation to which the difference scheme provides a better approximation. For details on how to fully obtain the modified equation for finite difference schemes we refer to [1] and [12].

The modified equation for the Lax-Friedrichs and first order upwind numerical schemes can be written in the form

$$u_t + a(u)u_x = Du_{xx} \tag{3.30}$$

where

$$D = \frac{1}{2}\Delta x\left(1 - a\frac{\Delta t}{\Delta x}\right)\left(1 + \frac{\Delta x}{a\Delta t}\right) \tag{3.31}$$

and

$$D = \frac{1}{2}\Delta x\left(1 - a\frac{\Delta t}{\Delta x}\right), \tag{3.32}$$

respectively. Examination of these two equations by using Fourier Transforms [12], shows the schemes to be of a non-dispersive nature, due to the waves travelling at the same speed as of those in equation (1.1). The CFL number $a\frac{\Delta t}{\Delta x}$ is positive and at most 1, so when $D > 0$ the amplitudes of the waves are damped with the higher wave numbers being affected more severely. Therefore we can conclude that the Lax- Friedrichs and first order upwind schemes are dissipative. By looking at equations (3.31) and (3.32) we can clearly see that the coefficient for the Lax- Friedrichs scheme has a much larger factor than of the first order upwind scheme, so we expect the Lax-Friedrichs scheme to be much more diffusive than the first order upwind scheme.

The modified equation for the Lax-Wendroff and Warming-Beam numerical schemes can be written in the form

$$u_t + a(u)u_x = Ru_{xxx} \tag{3.33}$$

where

$$R = \frac{1}{6}\Delta x^2\left(a^2\frac{\Delta t^2}{\Delta x^2} - 1\right) \tag{3.34}$$

and

$$R = \frac{1}{6}\Delta x^2\left(2 - a\frac{\Delta t}{\Delta x}\right)\left(1 - a^2\frac{\Delta t^2}{\Delta x^2}\right) \tag{3.35}$$

respectively. Investigation of equation (3.33) by Fourier Transforms shows that different wave numbers are travelling at different speeds, which means that the equation is said to be dispersive. By looking at the stability region for the Lax-Wendroff scheme, we can see that R is negative, which leads to high wave numbers travelling

with slower speed than they should. As a result of this we obtain oscillations occurring to the left of a shock. Due to the comparison of clasical numerical schemes, we shall concentrate on the lower half of the stability region $\left(0 \leq a\frac{\Delta t}{\Delta x} \leq 1\right)$ for the Warming-Beam scheme. If we consider the lower half of the stability region, by looking at equation (3.35) we can see that R will always stay positive. This resulting in high wave numbers travelling with faster velocity than they should, therefore the oscillations are observed in the front of the discontinuity for the Warming-Beam scheme.

Numerical results for the application of the schemes for Burgers and the Buckley-Leverett equations will be shown in chapter 5.

Chapter 4

Discontinuous Galerkin Method

In this Chapter we describe the derivation of the Discontinuous Galerkin Method, a non-classical method, and its application to the Buckley-Leverett equation.

4.1 Basic derivation of D-G Method

Given

$$u_t + f(u)_x = 0, \qquad in \qquad (a,b) \times (0,T) \tag{4.1}$$

with an initial condition

$$u(x,0) = u_0(x), \forall x \in (a,b) \tag{4.2}$$

To numerically solve equations (4.1) and (4.2), we can use the Discontinuous Galerkin method to discretise in space with a Runge-Kutta method to step forward in time [4] and [5]. We shall first discretize (4.1) and (4.2) in the spatial variable x. To discretize in space we proceed as follows. For each part of the interval (a,b), we set

$I_j = (x_{j-\frac{1}{2}}, x_{j+\frac{1}{2}})$ where $\Delta_j = x_{j+\frac{1}{2}} - x_{j-\frac{1}{2}}$ for $j = 1, \ldots, N$ and denote the quantity $max_{1\leq j\leq N}\Delta_j$ by Δx. We use the Galerkin method for which the finite dimensional space V_h to which the approximate solution $u^h(t)$ belongs to is taken as

$$V_h = V_h^k = \left\{ v \in L_1(0,1) : v \mid i_j \in P^k(I_J), j = 1, \ldots, N \right\}$$

where $P^k(I_j)$ denotes the space of polynomials of degree at most k in the cell (I_j). In V_h^k, the functions are allowed to have jumps at the interfaces $x_{j+\frac{1}{2}}$ which is why this method is called the Discontinuous Galerkin method. Multiply equation (4.1) by v and integrate over I_j,

$$\int_{I_j} v u_t dx + \int_{I_j} v f(u)_x dx = 0. \tag{4.3}$$

Integrating the second term by parts, gives

$$\int_{I_j} v u_t dx + \Big[v f(u) \Big]\Big|_{I_j} - \int_{I_j} v_x f(u) dx = 0 \tag{4.4}$$

Equation (4.4) is the weak form used for linear approximation. For each j put $u = u_0 + (x - x_{j-\frac{1}{2}})u_1$ and choose $v_0 = 1$ and $v_1 = (x - x_{j-\frac{1}{2}})$. Substituting $v_0 = 1$ into equation (4.4), yields

$$\int_{I_j} u_t dx + \left[f(u) \right]\Big|_{I_j} = 0. \tag{4.5}$$

Substituting $v_1 = (x - x_{j-\frac{1}{2}})$ into equation (4.4) we get

$$\int_{I_j} (x - x_{j-\frac{1}{2}}) u_t dx + \left[(x - x_{j-\frac{1}{2}}) f(u) \right]\Big|_{I_j} - \int_{I_j} f(u) dx = 0 \tag{4.6}$$

Equations (4.5) and (4.6) for all the $j's$ can be written in a concise ODE form

$$\frac{d}{dt}u_h = L_h(u^h) \tag{4.7}$$

where u_h is now the vector of (u_0, u_1)'s for all j. From figure 4.1 we can see that

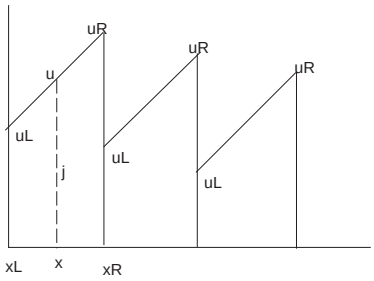

Figure 4.1: Graph to visualise the situation

$$u = u_L\left(\frac{x_R - x}{x_R - x_L}\right) + u_R\left(\frac{x - x_L}{x_R - x_L}\right)$$

$$= u_L(t)\phi_L(x) + u_R(t)\phi_R(x)$$

where

$$\phi_L = \left(\frac{x_{j+\frac{1}{2}} - x}{x_{j+\frac{1}{2}} - x_{j-\frac{1}{2}}}\right), \qquad \phi_R = \left(\frac{x - x_{j-\frac{1}{2}}}{x_{j+\frac{1}{2}} - x_{j-\frac{1}{2}}}\right)$$

which leads to

$$u_t = \frac{du_L}{dt}\phi_L(x) + \frac{du_R}{dt}\phi_R(x)$$

4.2 Buckley-Leverett flux

Introducing the Buckley - Leverett flux into equation (4.5) gives

$$\int_{I_j} u_t dx + \left[\frac{u^2}{u^2 + \frac{1}{4}(1-u)^2}\right]\Bigg|_{I_j} = 0 \tag{4.8}$$

Introducing the flux into equation (4.6) gives

$$\int_{I_j} (x - x_{j-\frac{1}{2}}) u_t dx + \left[(x - x_{j-\frac{1}{2}})\left(\frac{u^2}{u^2 + \frac{1}{4}(1-u)^2}\right)\right]\Bigg|_{I_j} - \int_{I_j}\left(\frac{u^2}{u^2 + \frac{1}{4}(1-u)^2}\right) dx = 0 \tag{4.9}$$

To evaluate the first term of equation (4.8), we proceed as follows

$$\int_{x_L}^{x_R} u_t dx = \int_{I_j}\left(\frac{du_L}{dt}\phi_L(x) + \frac{du_R}{dt}\phi_R(x)\right) dx$$

$$= \frac{du_L}{dt}\int_{x_L}^{x_R}\left(\frac{x_R - x}{x_R - x_L}\right) dx + \frac{du_R}{dt}\int_{x_L}^{x_R}\left(\frac{x - x_L}{x_R - x_L}\right) dx$$

By integrating we obtain

$$\int_{x_L}^{x_R} u_t dx = \frac{du_R}{dt}\frac{1}{x_R - x_L}\left[\frac{1}{2}\big(x - x_L)\big)^2\right]_{x_L}^{x_R} + \frac{du_L}{dt}\frac{1}{x_R - x_L}\left[\frac{1}{2}\big(x_R - x)\big)^2\right]_{x_L}^{x_R}$$

Substituting in the limits we obtain

$$\int_{x_L}^{x_R} u_t dx = \frac{du_R}{dt}\frac{1}{2}\big(x_R - x_L\big) + \frac{du_L}{dt}\frac{1}{2}\big(x_L - x_R\big). \tag{4.10}$$

To evaluate the second term of equation (4.8), we have to treat this term in a special way, to do this we proceed as follows

$$\Big[f\big(u\big)\Big]\Big|_{I_j} = \Big(f\big(u_{j+\frac{1}{2}}\big) - f\big(u_{j-\frac{1}{2}}\big)\Big)$$

Replacing the non-linear flux $f\Big(u\big(x_{j+\frac{1}{2}},t\big)\Big)$ by a numerical flux which depends on two values of u_h at the point $\big(x_{j+\frac{1}{2}},t\big)$, this is given by

$$h(u)_{j+\frac{1}{2}}(t) = h\big(u(x^-_{j+\frac{1}{2}},t)(u(x^+_{j+\frac{1}{2}},t)\big)$$

By using a monotone numerical flux, we should achieve high-order accuracy while keeping their stability and convergence properties. A monotone flux is one which satisfies the following properties listed below.

- If it is locally Lipschitz and consistent with the flux $f(u)$, for example $h(u,u) = f(u)$.
- If it is a nondecreasing function of its first argument, and a nonincreasing function of its second argument

An example of a numerical flux which satisfies the above properties is the Local Lax-Friedrichs flux, which is given by

$$h^{LLF}\big(a,b\big) = \frac{1}{2}\Big[f(a) + f(b) - C(b-a)\Big] \tag{4.11}$$

where $a = u(x^-_{j+\frac{1}{2}},t)$ and $b = u(x^+_{j+\frac{1}{2}},t)$ and $C = Max_{min(a,b)\leq u\leq max(a,b)}\Big|f'(u)\Big|$. Applying the formula to the Buckley-Leverett flux we obtain

$$h^{LLF} = \frac{1}{2}\left(\frac{u^{-2}_{j+\frac{1}{2}}}{u^{-2}_{j+\frac{1}{2}} + \frac{1}{4}\big(1-u^-_{j+\frac{1}{2}}\big)^2}\right) - \frac{1}{2}\left(\frac{u^{-2}_{j-\frac{1}{2}}}{u^{-2}_{j-\frac{1}{2}} + \frac{1}{4}\big(1-u^-_{j-\frac{1}{2}}\big)^2}\right) + \frac{1}{2}\left(\frac{u^{+2}_{j+\frac{1}{2}}}{u^{+2}_{j+\frac{1}{2}} + \frac{1}{4}\big(1-u^+_{j+\frac{1}{2}}\big)^2}\right)$$

$$-\frac{1}{2}\left(\frac{u^{+2}_{j-\frac{1}{2}}}{u^{+2}_{j-\frac{1}{2}}+\frac{1}{4}\left(1-u^{+}_{j-\frac{1}{2}}\right)^2}\right)-\frac{1}{2}C\left(u^{+}_{j+\frac{1}{2}}-u^{-}_{j+\frac{1}{2}}\right)+\frac{1}{2}C\left(u^{+}_{j-\frac{1}{2}}-u^{-}_{j-\frac{1}{2}}\right)$$

To evaluate the first term of equation (4.9), we proceed as follows

$$\int_{x_L}^{x_R}(x-x_L)u_t dx=\int_{x_L}^{x_R}(x-x_L)\left(\frac{du_L}{dt}\phi_L(x)+\frac{du_R}{dt}\phi_R(x)\right)dx$$

$$=\frac{du_L}{dt}\int_{x_L}^{x_R}(x-x_L)\left(\frac{x_R-x}{x_R-x_L}\right)dx+\frac{du_R}{dt}\int_{x_L}^{x_R}(x-x_L)\left(\frac{x-x_L}{x_R-x_L}\right)dx$$

By integrating we obtain

$$\int_{x_L}^{x_R}(x-x_L)u_t dx=\frac{du_R}{dt}\frac{1}{x_R-x_L}\left[\frac{1}{3}\left(x-x_L\right)^3\right]_{x_L}^{x_R}+\frac{du_L}{dt}\frac{1}{x_R-x_L}\left[\frac{x_R x^2}{2}-x_L x_R x-\frac{x^3}{3}+\frac{x_L x^2}{2}\right]_{x_L}^{x_R}$$

hence

$$\int_{x_L}^{x_R}(x-x_L)u_t dx=\frac{du_R}{dt}\left[\frac{1}{3}\left(x_R-x_L\right)^2\right]+\frac{du_L}{dt}\frac{1}{x_R-x_L}\left[\frac{1}{6}x_R^3-\frac{1}{2}x_L x_R^2-\frac{1}{6}x_L^3+\frac{1}{2}x_R x_L^2\right]$$

To evaluate the second term of equation (4.9), we treat this term in the same way as we did previously for the second term in equation (4.8). By doing this we obtain

$$\left[(x-x_{j-\frac{1}{2}})f(u)\right]_{j-\frac{1}{2}}^{j+\frac{1}{2}}=\left(x_{j+\frac{1}{2}}-x_{j-\frac{1}{2}}\right)\left(f\left(u_{j+\frac{1}{2}}\right)\right)$$

Applying the Local-Lax Friedrichs flux to this term yields

$$h^{LLF}=\frac{1}{2}\left(x_{j+\frac{1}{2}}-x_{j-\frac{1}{2}}\right)\left(\frac{u^{-2}_{j+\frac{1}{2}}}{u^{-2}_{j+\frac{1}{2}}+\frac{1}{4}\left(1-u^{-}_{j+\frac{1}{2}}\right)^2}\right)+\frac{1}{2}\left(x_{j+\frac{1}{2}}-x_{j+\frac{1}{2}}\right)\left(\frac{u^{+2}_{j+\frac{1}{2}}}{u^{+2}_{j+\frac{1}{2}}+\frac{1}{4}\left(1-u^{+}_{j+\frac{1}{2}}\right)^2}\right)$$

$$-\frac{1}{2}\big(x_{j+\frac{1}{2}}-x_{j-\frac{1}{2}}\big)\big(\frac{1}{3}\big(x_{j+\frac{1}{2}}-x_{j-\frac{1}{2}}\big)^2\big)\left(u^+_{j+\frac{1}{2}}-u^-_{j+\frac{1}{2}}\right)$$

We are now left with the final term in equation (4.9). To integrate this we use Gaussian Quadrature. To evaluate Lu we have to solve the 2 simultaneous equations

$$A\frac{du_R}{dt}+B\frac{du_L}{dt}=RHS1 \tag{4.12}$$

and

$$C\frac{du_R}{dt}+D\frac{du_L}{dt}=RHS2, \tag{4.13}$$

where

$$RHS1=\frac{1}{2}\left(\frac{u^{-2}_{j+\frac{1}{2}}}{u^{-2}_{j+\frac{1}{2}}+\frac{1}{4}\big(1-u^-_{j+\frac{1}{2}}\big)^2}\right)-\frac{1}{2}\left(\frac{u^{-2}_{j-\frac{1}{2}}}{u^{-2}_{j-\frac{1}{2}}+\frac{1}{4}\big(1-u^-_{j-\frac{1}{2}}\big)^2}\right)+\frac{1}{2}\left(\frac{u^{+2}_{j+\frac{1}{2}}}{u^{+2}_{j+\frac{1}{2}}+\frac{1}{4}\big(1-u^+_{j+\frac{1}{2}}\big)^2}\right)$$

$$-\frac{1}{2}\left(\frac{u^{+2}_{j-\frac{1}{2}}}{u^{+2}_{j-\frac{1}{2}}+\frac{1}{4}\big(1-u^+_{j-\frac{1}{2}}\big)^2}\right)-\frac{1}{2}C\left(u^+_{j+\frac{1}{2}}-u^-_{j+\frac{1}{2}}\right)+\frac{1}{2}C\left(u^+_{j-\frac{1}{2}}-u^-_{j-\frac{1}{2}}\right)$$

$$RHS2=\frac{1}{2}\big(x_{j+\frac{1}{2}}-x_{j-\frac{1}{2}}\big)\left(\frac{u^{-2}_{j+\frac{1}{2}}}{u^{-2}_{j+\frac{1}{2}}+\frac{1}{4}\big(1-u^-_{j+\frac{1}{2}}\big)^2}\right)+\frac{1}{2}\big(x_{j+\frac{1}{2}}-x_{j+\frac{1}{2}}\big)\left(\frac{u^{+2}_{j+\frac{1}{2}}}{u^{+2}_{j+\frac{1}{2}}+\frac{1}{4}\big(1-u^+_{j+\frac{1}{2}}\big)^2}\right)$$

$$-\frac{1}{2}\big(x_{j+\frac{1}{2}}-x_{j-\frac{1}{2}}\big)C\left(u^+_{j+\frac{1}{2}}-u^-_{j+\frac{1}{2}}\right)+Gaussian\ Quadrature\ part$$

and

$$A=\frac{1}{2}\big(x_{j+\frac{1}{2}}-x_{j-\frac{1}{2}}\big),\qquad B=\frac{1}{2}\big(x_{j-\frac{1}{2}}-x_{j+\frac{1}{2}}\big),\qquad C=\frac{1}{3}\big(x_{j+\frac{1}{2}}-x_{j-\frac{1}{2}}\big)^2$$

$$D=\left[\frac{1}{6}x^3_{(j+\frac{1}{2})}-\frac{1}{2}x_{(j-\frac{1}{2})}x^2_{(j+\frac{1}{2})}-\frac{1}{6}x^3_{(j-\frac{1}{2})}+\frac{1}{2}x_{(j+\frac{1}{2})}x^2_{(j-\frac{1}{2})}\right]$$

Solving equations (4.12) and (4.13) simultaneously yields

$$\frac{du_L}{dt} = \frac{C * RHS1 - A * RHS2}{B * C - A * D} \tag{4.14}$$

and

$$\frac{du_R}{dt} = \frac{RHS1}{A} - B\frac{(RHS1 - A * RHS2)}{A(B * C - A * D)} \tag{4.15}$$

We can now apply the TVD-Runge-Kutta to discretise our ODE system in time [2]. If $\left(t^n\right)_{n=0}^N$ is a partition of $[0, T]$ and $\Delta t^n = t^{n+1} - t^n, n = 0, \cdots, N-1$, then our time marching algorithm reads as follows:

- Set $u_h^0 = u_h^n$;
- For $n = 0, \cdots, N-1$ compute u_h^{n+1} from u_h^n as follows:

1 Set $u_h^0 = u_h^n$;

2 for $i = 1, \cdots, k+1$ compute the intermediate functions:

$$u_h^i = \left(\sum_{l=0}^{i-1} \alpha_{il} u_h^l + \beta_{il} \Delta t^n L_h\left(u_h^l\right) \right); \tag{4.16}$$

3 set $u_h^{n+1} = u_h^{(k+1)}$.

where $L_h\left(u_h^l\right)$ is given by equations (4.14) and (4.15). In equation (4.16) we take k to equal one, where α_{il} and β_{il} are the Runge-Kutta time discretisation parameters.

Chapter 5

Numerical Results

Numerical experiments were performed using five different numerical schemes. The schemes used are the first order upwind, Lax-Friedrichs, Lax- Wendroff, Warming-Beam and the Runge-Kutta Discontinuous Galerkin method. Unfortunately we could not get the RKDG program to work, so used one kindly made available by Paul Jelfs. The Burgers and Buckley-Leverett equations were used,

$$u_t + \left(\frac{1}{2}u^2\right)_x = 0 \tag{5.1}$$

and

$$u_t + \left(\frac{u^2}{u^2 + \frac{1}{4}(1-u)^2}\right)_x = 0 \tag{5.2}$$

respectively. Equations (5.1) and (5.2) were tested with different initial boundary conditions to check the behaviour and accuracy of the numerical schemes.

5.1 Burgers initial data 1

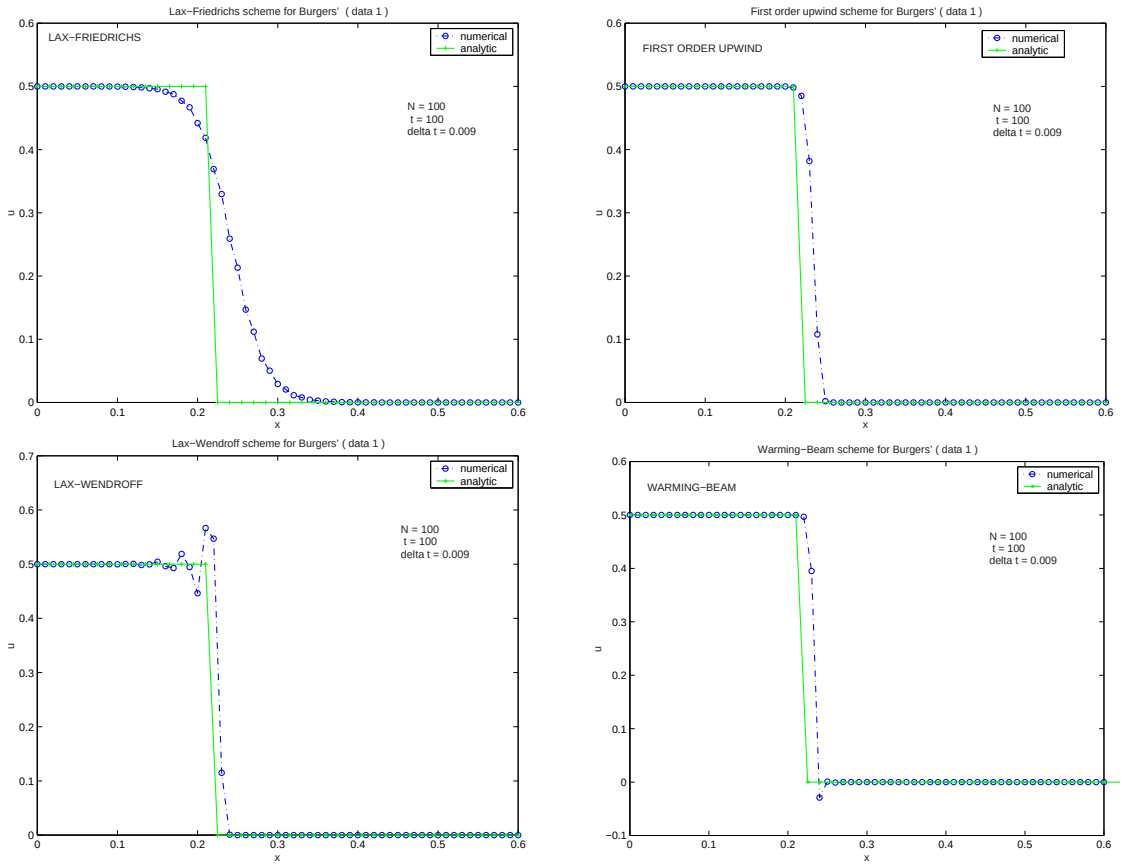

Figure 5.1: Graphs of schemes for Burgers' initial data 1 points

The solution for this data describes a shock which is propagating in the positive x-direction, with a speed of 0.25. We can compare the behaviour of the numerical schemes, since the analytic solution is known. Figures (5.1) and (5.2) were plotted using a step size $\Delta x = 0.01$ and a time step $\Delta t = 0.009$, with a number of 100 timesteps used for figure (5.1). At this particular time point the shock has moved to $x = 0.225$ from its initial position. By analysing fig (5.1) we can clearly see that the Lax-Friedrichs and the first order upwind schemes have introduced numerical

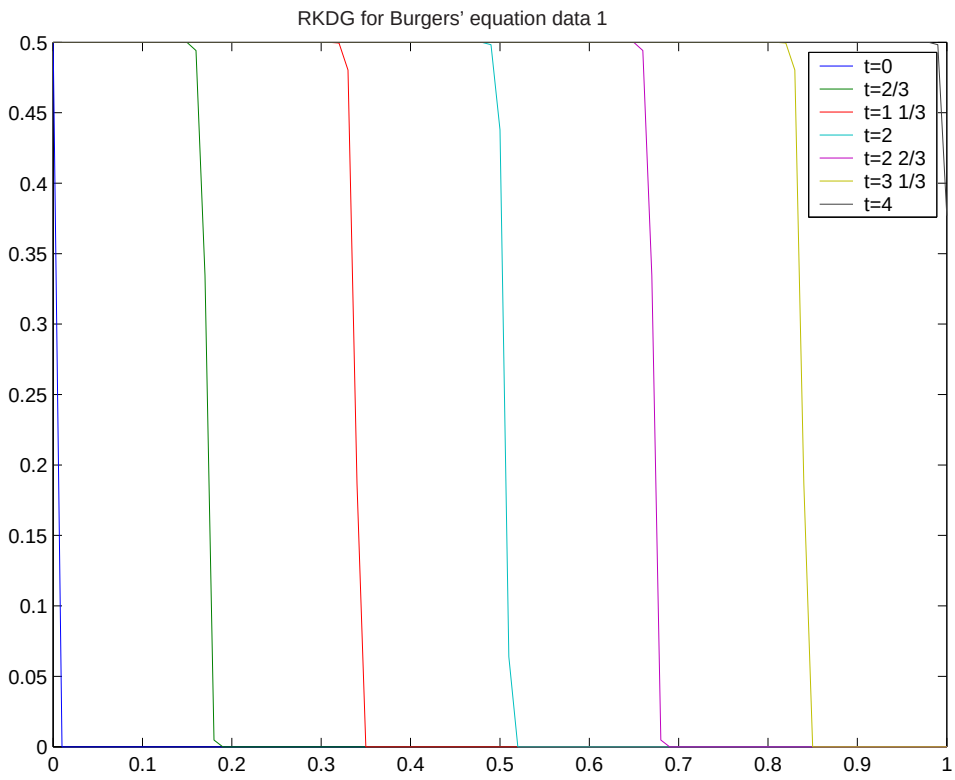

Figure 5.2: Graph of RKDG method for Burgers equation with initial data 1

diffusion (smearing). The smearing for the Lax-Friedrichs scheme is much more severe than of the first order upwind scheme, this being a direct feature of the truncation error terms of these schemes (see Chapter 3), whilst the Lax-Wendroff and Warming-Beam schemes are much more accurate at capturing the shock. The Lax-Wendroff scheme produces spurious oscillations to the left of the shock and the Warming-Beam scheme creates oscillations to the right of the shock, as can be seen by looking at figure (5.1). Finally by looking at figure (5.2) we can see that the RKDG method does not create oscillations, due to the use of the TVD Runge-Kutta to march forward in time. However, there is a subtle smearing if we look at the time intervals provided on the graph.

5.2 Burgers initial data 2

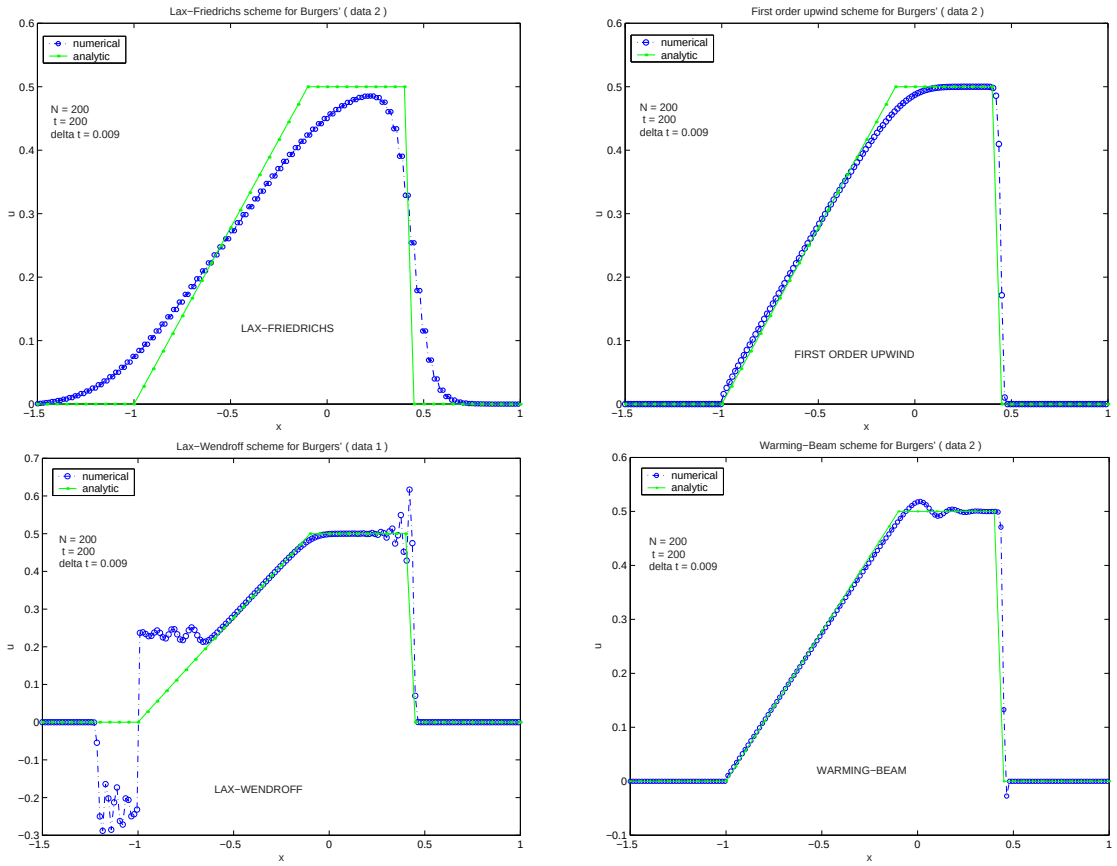

Figure 5.3: Graphs for Burgers' initial data 2 points

The solution for this data describes an expansion fan which has a fixed initial boundary condition at $x = -1$, and the final boundary condition is infinite. The fan which is present eventually meets up with the shock at the location time $t = 4$ at the interval $x = 1$. Figure (5.3) was plotted using a step size $\Delta x = 0.0125$ and a time step of $\Delta t = 0.009$, with 200 timesteps, giving a location time of 1.8 where the expansion fan and shock yet to meet. By looking at figure (5.3), we can see that the Lax-Friedrichs scheme has introduced some severe numerical diffusion,

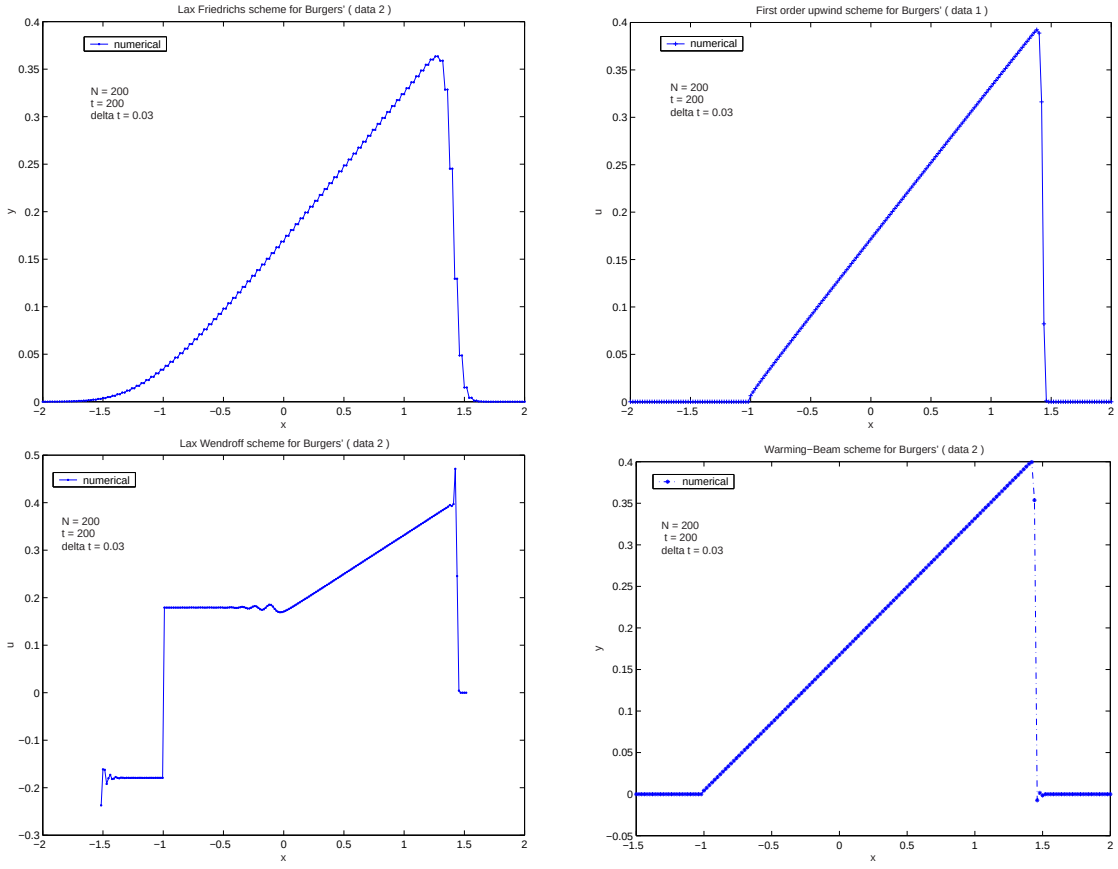

Figure 5.4: Graphs for Burgers' initial data 2 points

which has influenced the accuracy of the scheme compared to the analytical solution. The first order upwind scheme has behaved somewhat better, with better accuracy than of the Lax-Friedrichs scheme. The Lax-Wendroff and Warming-Beam schemes are the most accurate of the four classical schemes, but the overall phase shape is quite poor, due to introduction of oscillations which are present behind and front of the discontinuities, respectively. The behaviour to the left of the fan for the Lax-Wendroff scheme is due to entropy violation. Figure (5.4) was plotted using a step size $\Delta x = 0.02$ and a time step of $\Delta t = 0.03$, with 200 timesteps,

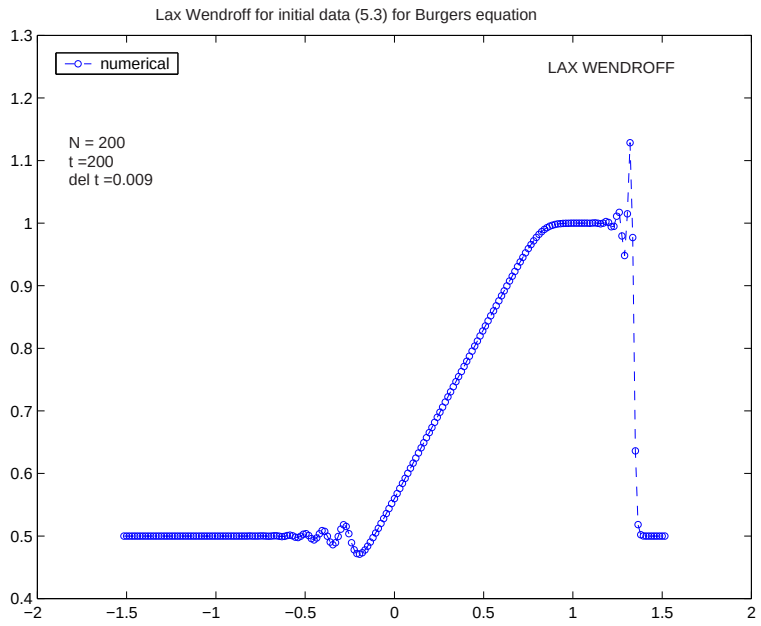

Figure 5.5: Graph for Lax Wendroff scheme with initial data (5.3)

giving a location time of 6. At this time the expansion fan and the shock are combined together. By looking at figure (5.4), we can clearly see that by moving forward in time, the initial square wave has been damped, this being a feature of the shock and fan combining together. Once again the Lax-Friedrich scheme is the most dissipative in comparison to the first order upwind scheme, both of the schemes giving poor resolution to discontinuities. Although the Lax-Wendroff and Warming-Beam schemes are creating oscillations, the position of the final location of the shock are most accurate.

If we change initial data 2 and use the initial conditions

$$u(x,0) = \begin{cases} 0.5 & x < -1 \\ 1 & -1 < x < 0 \\ 0.5 & x > 0 \end{cases} \tag{5.3}$$

we do not obtain the entropy violation as occurred in figures (5.3) and (5.4) for the Lax-Wendroff scheme. Figure (5.5) was plotted using a step size $\Delta x = 0.0125$ and a time step of $\Delta t = 0.009$, with 200 timesteps. By looking at this figure we can clearly see that the problem we faced earlier has been resolved. The graph shows that at the discontinuities, the oscillations are behind the shock and the expansion fan.

5.3 Buckley - Leverett initial data 1

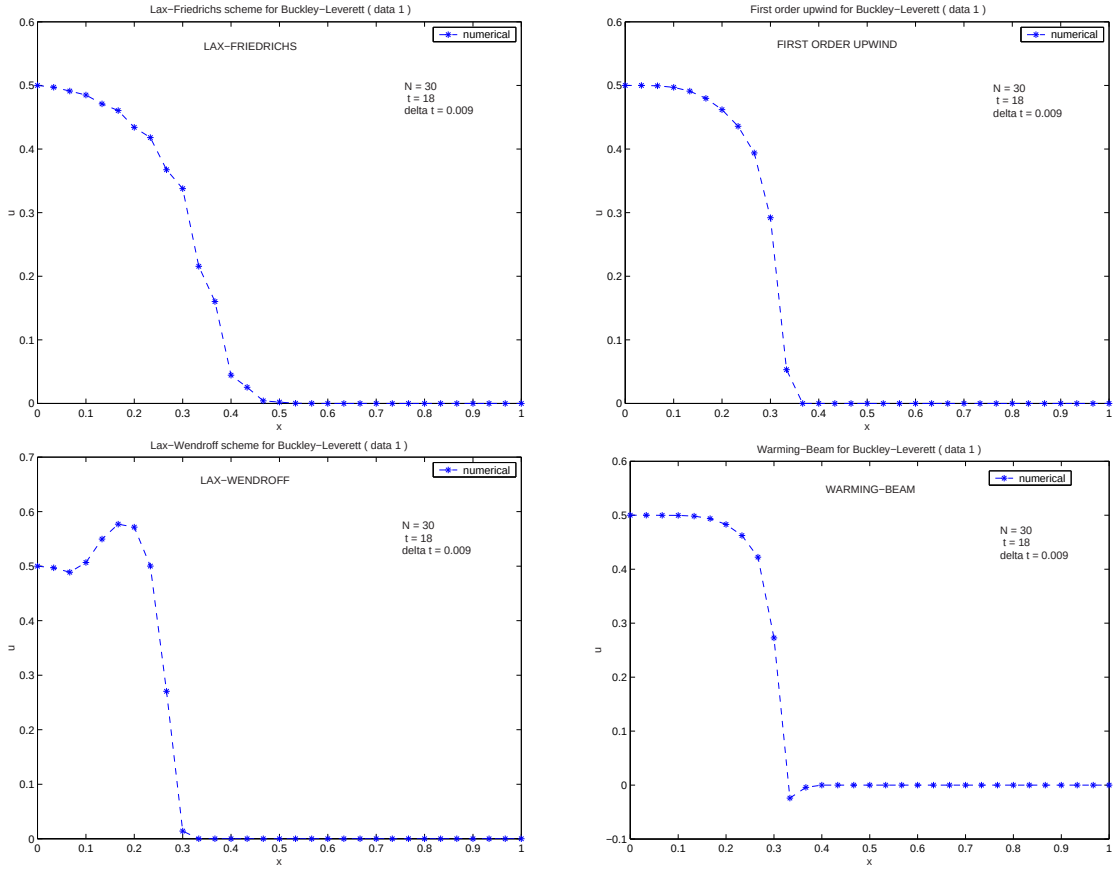

Figure 5.6: Graphs for Buckley-Leverett using initial data 1

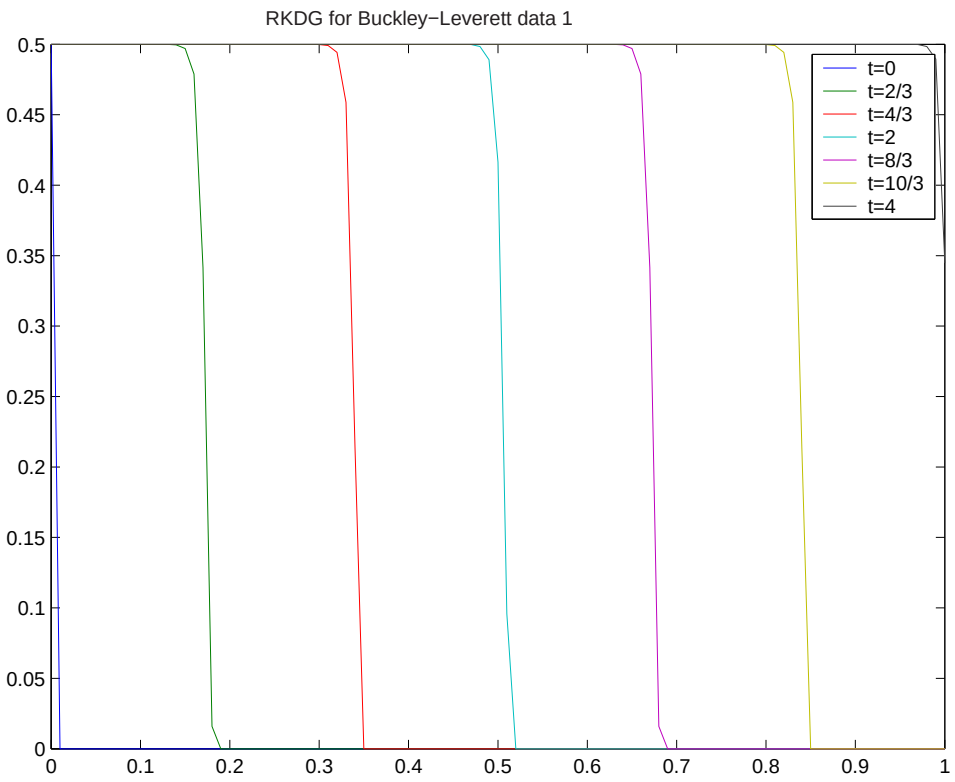

Figure 5.7: Graph for Buckley-Leverett using RKDG method for initial data 1

The solution for this data for the Buckley-Leverett equation should show a shock travelling in the positive x-direction, with a speed of 1.6. Figures (5.6) and (5.7) was plotted using a step size $\Delta x = 0.033$ and a time step $\Delta t = 0.009$, where the number of timesteps used is 18 for figure (5.6). At this particular time point the shock should have moved to $x = 0.26$ from its initial position.

By analysing the results given by figure (5.6), we can deduce that the Lax-Friedrichs scheme is more diffusive than the first order upwind as initially expected. The Lax-Wendroff and Warming-Beam schemes are again the most accurate, but produce oscillations to the left and right of the discontinuity, respectively. This is a feature

of these type of second order numerical schemes. By looking at figure (5.7), we can see that the waves for the RKDG method seem to be travelling way too slow. However by extracting the behaviour from these results, we can visualise that there are no oscillations present due to the built in TVD property.

5.4 Buckley - Leverett initial data 2

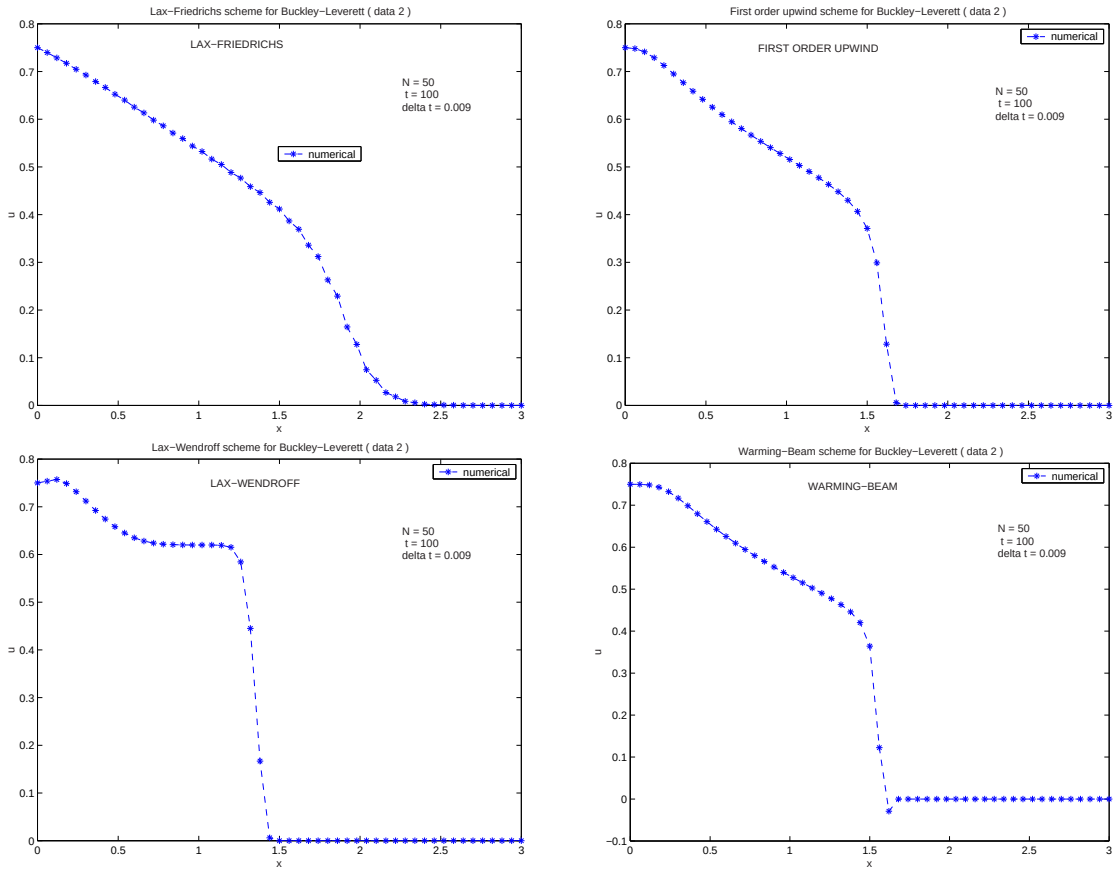

Figure 5.8: Graphs for Buckley-Leverett using initial data 2

This initial data generates a fan and a shock conbination. Figures (5.8) and (5.9) was plotted using a step size $\Delta x = 0.06$ and a time step $\Delta t = 0.009$, where the

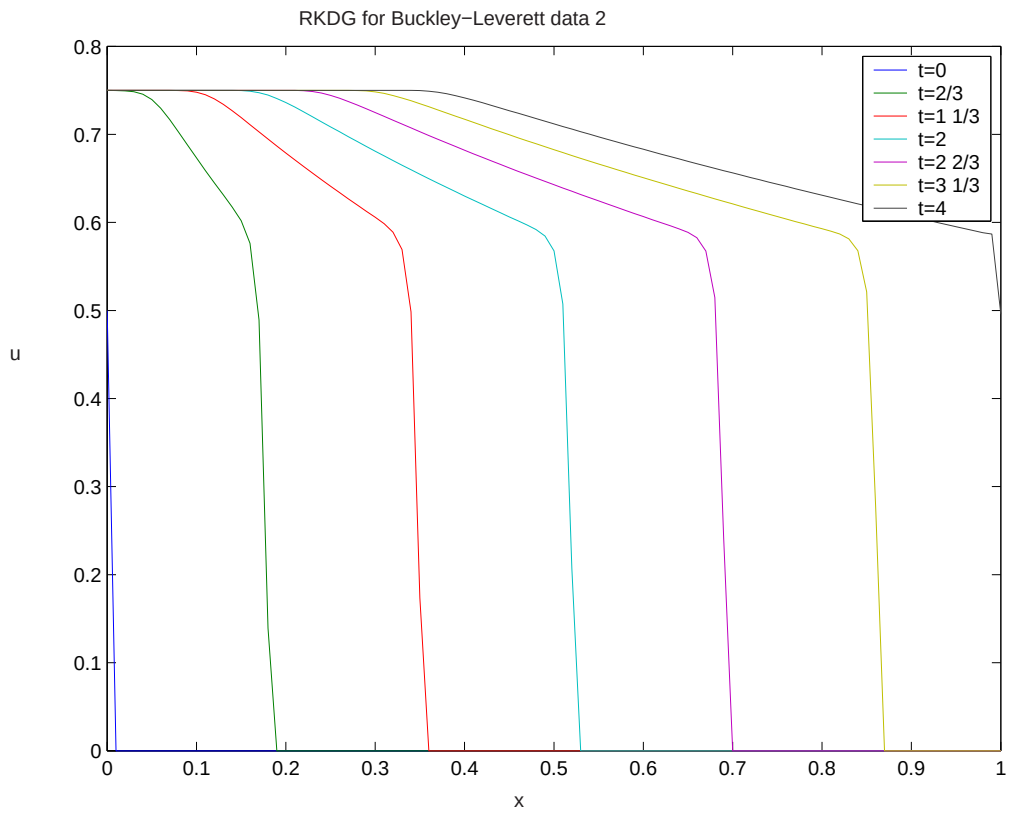

Figure 5.9: RKDG for Buckley-Leverett initial data 2

number of timesteps is 100 for figure (5.8). From the results obtained in figure (5.8) we can clearly see that the Lax-Friedrichs scheme is yet again the most diffusive, in comparison to the first order upwind scheme.

The Lax-Wendroff scheme for this initial data seems not to have produced any visible oscillations to the left of the shock. This is most probably due to the combination of the fan and the shock combining together at left of the shock, where the fan is damping the oscillations that are produced by the shock, therefore resulting with no visible oscillations to the left of the shock. By looking at the Warming-Beam scheme we can clearly see that oscillations are still present to the right of the shock

as initially expected. By looking at figure (5.9) we can see that the second order RKDG method has not produced any oscillations, although there is slight evidence of smearing, even though the speed of the waves are yet again moving way too slow.

Chapter 6

Conclusion

In this dissertation we have studied the effects of four classical schemes on the Burgers and Buckley-Leverett equations. The schemes are first order upwind, Lax-Friedrichs, Lax-Wendroff and Warming-Beam, found that the the Lax-Friedrichs and the first order upwind schemes are very diffusive, this being a common feature for first order accurate schemes. The reason for this type of dissipative behaviour is an artefact of the terms in the truncation error for these schemes.

The Lax-Wendroff, Warming-Beam and the RKDG method are second order accurate schemes, and it is a well known fact that second order accurate numerical schemes produce oscillations at discontinuities. The Lax-Wendroff scheme is shown to produce oscillations to the left of the discontinuities, except for initial data 2 for the Buckley-Leverett equation, where we had the fan and shock combination. The Warming-Beam scheme has produced oscillations to the right of the shock for all the cases considered. However the oscillations for the Lax-Wendroff and Warming-Beam schemes can be suppressed by using limiters, although that has not been done

here. The RKDG method does not introduce such oscillations, because the method implements the TVD property, which is sufficient to stop oscillations from occurring.

6.1 Further work

For further work we can modify the classical Lax-Wendroff and Warming-Beam schemes by introducing the flux limiter methods. By applying limiters, we can eliminate oscillations that are produced by these second order accurate schemes. This will enable us to develop high order resolution schemes, without the presence of spurious oscillations near discontinuities.

To construct the method [1] we let hG be the numerical flux of the second order accurate classical scheme, and we let hL be the numerical flux of a low order TVD scheme. If $hG(u^n_{j+k-1}, ...u^n_{j+k})$ and $hL(u^n_{j+k-1}, ...u^n_{j+k})$ are abbreviated by $hG(u^n_j)$ and $hL(u^n_j)$ respectively, the new method can now be written as

$$h(u^n_j) = hL(u^n_j) + \phi(u^n_j)\big(hG(u^n_j) - hL(u^n_j)\big)$$

where ϕ is called the limiter. The limiter has to act as a sensor for sudden strong increase or decrease of the unknown exact solution expected to occur at positions, where the numerical solution strongly increases or decreases with respect to space.

Bibliography

[1] R. Ansorge, "Mathematical Models of Fluiddynamics An Introduction", WILEY-VCH GmbH and co. KGaA, (2003).

[2] E.B. Becker, G.F. Carey and J.T. Oden. "finite elements: an introduction", Prentice-Hall, New Jersey, (1981).

[3] W. Cheney and D. Kincaid, "numerical mathematics and computing", Brooks/Cole publishing co, London, (2002).

[4] B. Cockburn and C.W. Shu, "A new class of non-oscillatory discontinuous Galerkin finite element methods for conservation laws", pp.977-986.

[5] B. Cockburn and C.W Shu, " Discontinuous Galerkin methods for convection dominated problems", J. Sci. Comput 16(2001), no.3, pp 173-261.

[6] P. Concus and W. Proskurowski, "Numerical solution of a non-linear hyperbolic equation by a random choice method", J.Comput. Phys, 30(1979), pp 153-166.

[7] A. Harten, "High Resolution Schemes for Hyperbolic Conservation Laws", J.Comput.Phys, 49(1983), pp 357-393.

[8] Y. Wang, and K. Hutter, "Comparison of numerical methods with respect to convectively dominated problems", Int. J. Meth. Fluids, 37(2001), pp 721-745.

[9] K.W. Morton and D.F. Mayers, "Numerical Solution of Partial Differential Equations". Cambridge university press, (1994).

[10] D. Potter, "Computational Physics" A Wiley - Interscience Publication, London, (1977).

[11] P.K Sweby, "High Resolution Schemes Using Flux Limiters for Hyperbolic Conservation Laws". SIAM J. Numerical. Anallysis, 21(5), pp 995-1101.

[12] P.K Sweby, "Numerical Solution of Conservation Laws" Lecture notes, University of Reading (2002).

[13] P.K Sweby, "Theory of Differential equations" Lecture notes, University of Reading (2002).

[14] A.J. Wathen, "Moving finite elements and reservoir modelling" PhD Thesis, Department of Mathematics, University of Reading , (1984).